# Deep–Inelastic ep Scattering at Very High $Q^2$

Ulrich F. Katz, ZEUS
University of Bonn*

Minerva–G.I.F. Gentner Symposium
From Elementary Particles to Complex Systems
Jerusalem, 25–28 May 1998

- Introduction
- DIS in the Standard Model
- Cross–Section Measurements
- Scenarios Beyond the Standard Model
- Conclusion and Outlook

Focus on cross–section measurements
Mainly new results (1994–1997 data)

---

*Temporarily with the University of Hamburg

# Introduction

HERA= first electron–proton collider

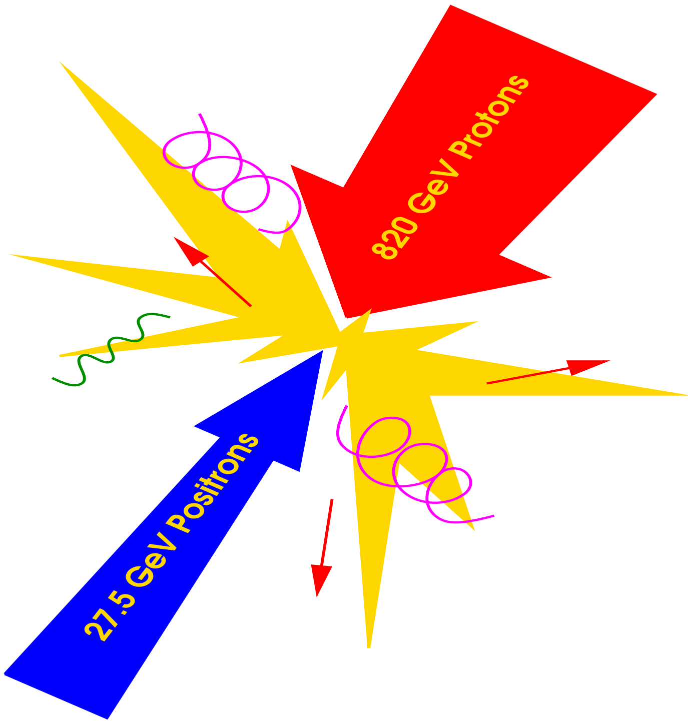


$ep$ centre–of–mass energy = 300 GeV
electron–quark invariant mass up to $\sim$ 200 GeV
spatial resolution $2 \cdot 10^{-16}$ cm
(at $Q^2 = 10^4$ GeV$^2$)
ZEUS 1994–1997 integrated $\mathcal{L} = 46.6\,\mathrm{pb}^{-1}$
H1 1994–1997 integrated $\mathcal{L} = 37.0\,\mathrm{pb}^{-1}$
$\longrightarrow$ sensitive to $\sigma \sim 50$ fb

# DIS Signatures and Kinematics

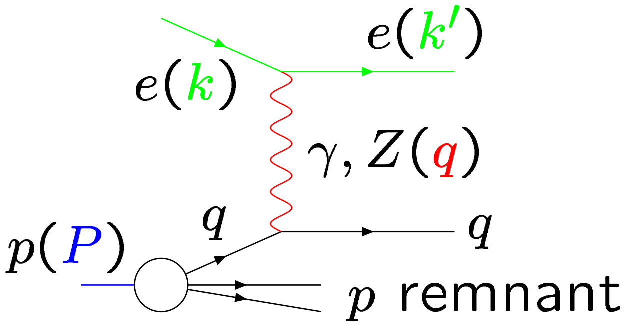


## Neutral Current (NC)

Scattered $e$ in main detector

$e$ balances hadronic $p_t$

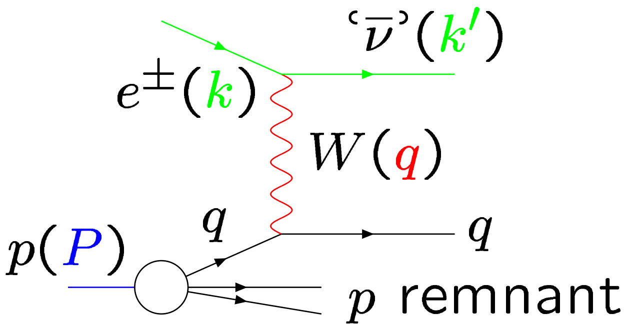


## Charged Current (CC)

Scattered $\nu$ invisible

Only hadronic system available for measurements

## Kinematic Variables:

Four–momentum transfer:

$$Q^2 = -q^2 = -(k - k')^2 = 2E_e E'(1 + \cos\theta_e)$$

Bjorken scaling variable:

$$x = Q^2/(2\,q \cdot P) = \text{momentum fraction of quark}$$

Inelasticity:

$$y = (q \cdot P)/(k \cdot P)$$

$$y = (1 - \cos\theta_e^*)/2; \quad \theta_e^* = eq \text{ c.m.s. scattering angle}$$

$ep$ centre-of-mass energy:

$$s = (k + P)^2 = 4E_e E_p$$

$eq$ invariant mass:

$$M = \sqrt{xs}$$

# The HERA Kinematic Plane

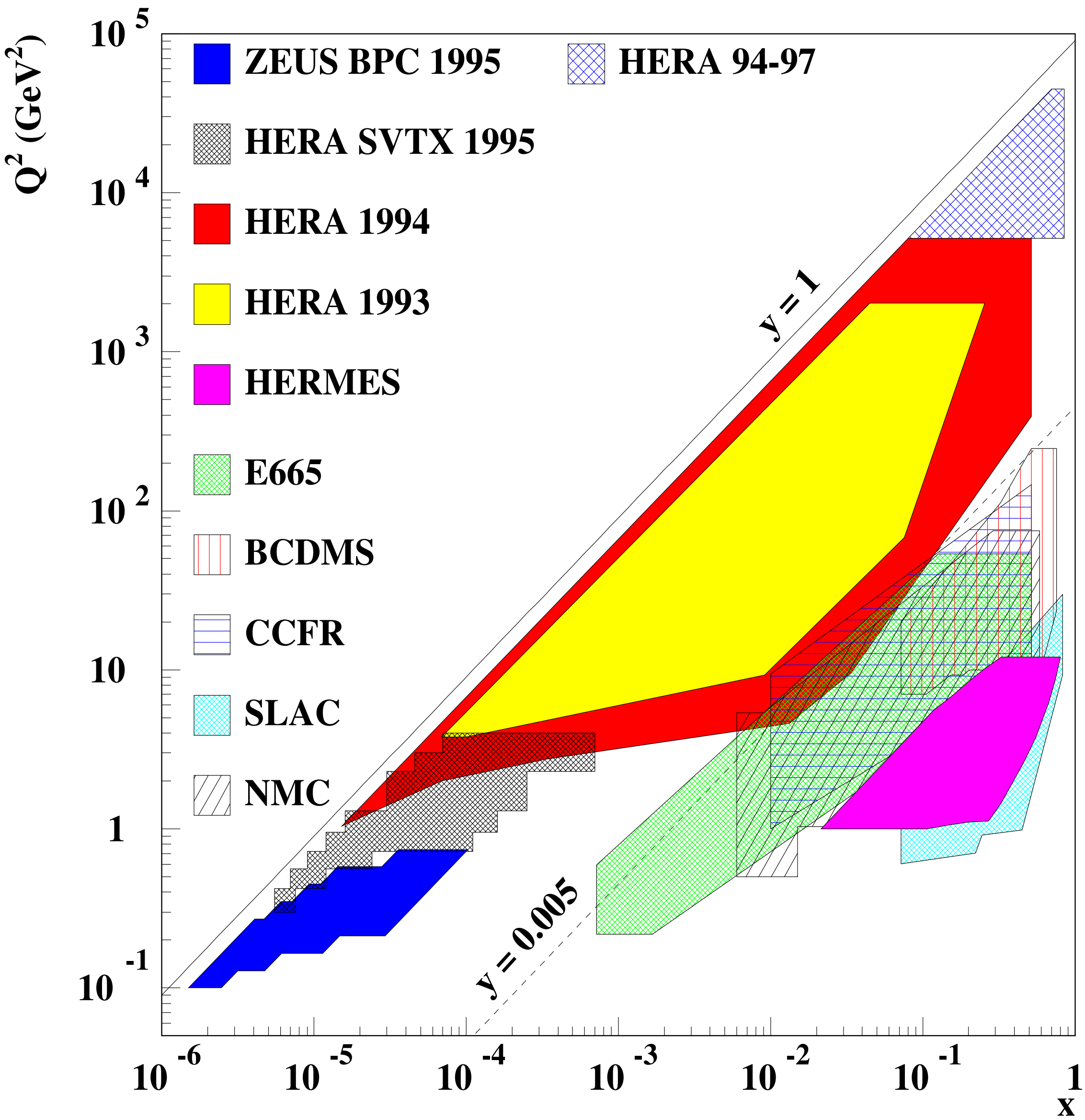


DIS at $Q^2 \gtrsim 5000\ \mathrm{GeV}^2$ became accessible with the high–statistics 1996+1997 $e^+p$ data

# High–$Q^2$ Event Topologies

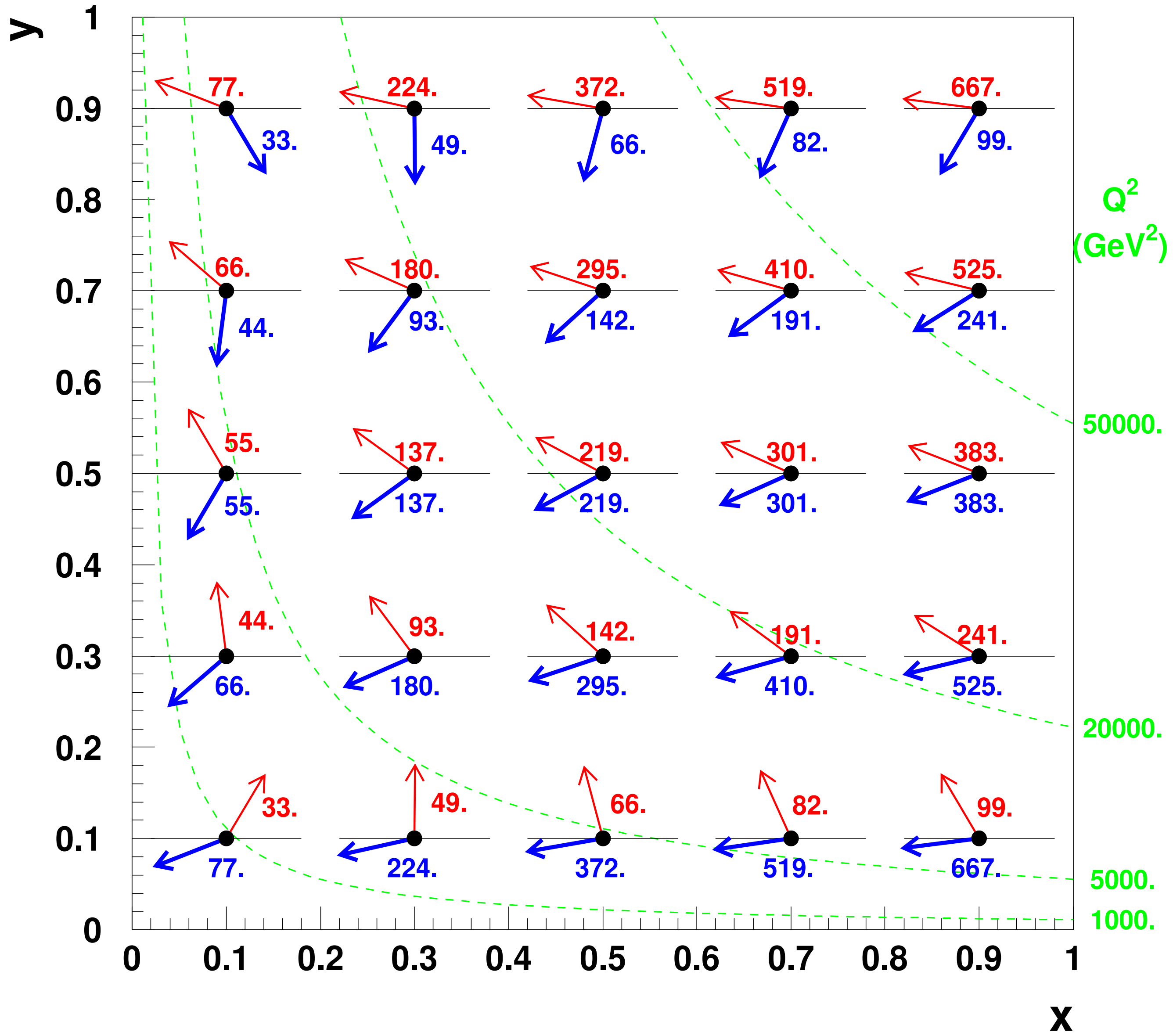


Final state topologies for elastic $eq \to eq$ scattering

Positrons enter from left, protons from right

Arrows = scattering angles of $e$ and $q$

Numbers = energies of scattered $e$ and $q$ (in GeV)

# A NC Event in the ZEUS Detector

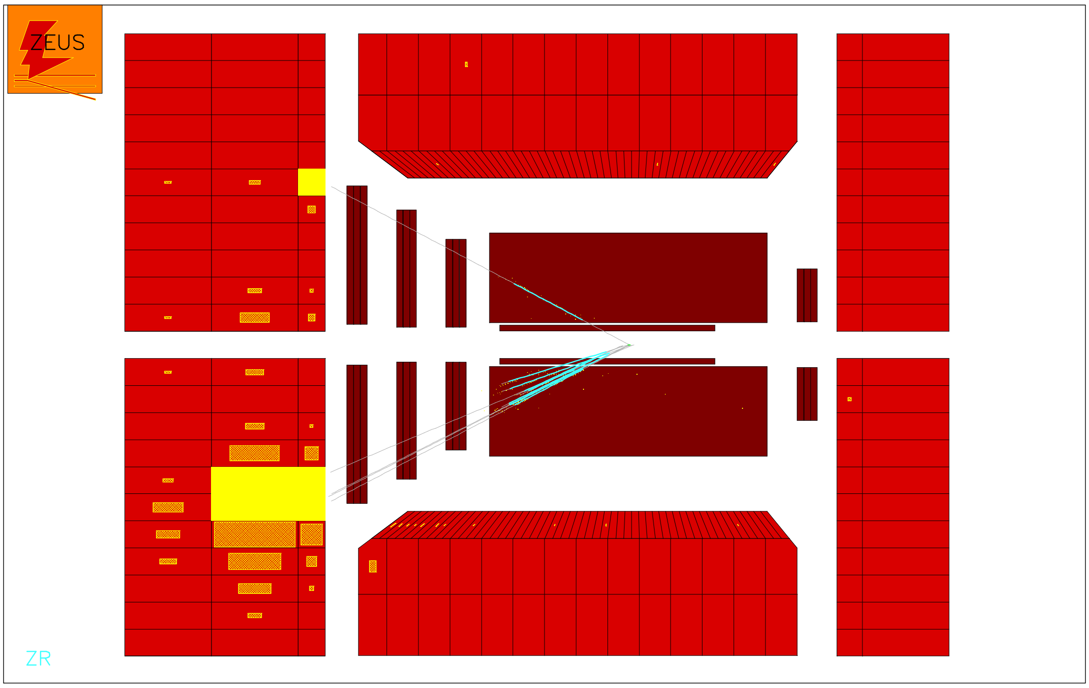


Uranium-Scintillator Calorimeter

6000 Cells, each read out by 2 PMTs

$$\sigma_{\theta_e} = 5 \text{ mrad}$$

$$\sigma/\sqrt{E} \text{ (e)} = 18 \%$$

$$\sigma/\sqrt{E} \text{ (had)} = 35 \%$$

$$\Delta E/E \text{ (syst)} = 3 \%$$

in situ calibration good to 1–2% (e)

# A CC Event in the H1 Detector

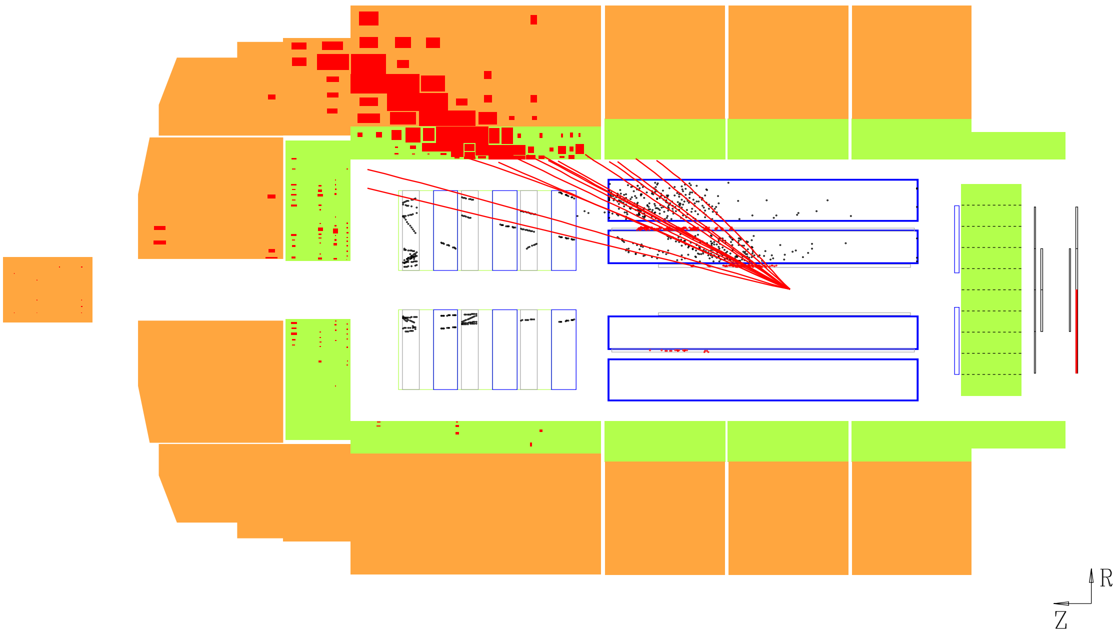


**Liquid Argon Calorimeter**

44000 Cells

$\sigma_{\theta_e}$ = 2-5 mrad

$\sigma/\sqrt{E}$ (e) = 12 %

$\sigma/\sqrt{E}$ (had) = 50 %

$\Delta E/E$ (syst) = 3 - 4 %

in situ calibration good to $1-3\%$ (e)

# DIS in the Standard Model

Deep–inelastic $ep$ scattering =
incoherent sum of elastic $eq$ scatterings

$$\boxed{\sigma(ep) = \sum_{q,\bar{q}} f_{q|p} \cdot \sigma(eq)}$$

## $f_{q|p} \equiv q =$ Parton distribution function (PDF)

Probability density to find quark $q$ in the proton
carrying a fraction $x$ of the proton momentum

Not predicted by theory

## $\sigma(eq) =$ electron–quark cross–section

Leading Order:

$\sigma(eq \to eq) \propto$

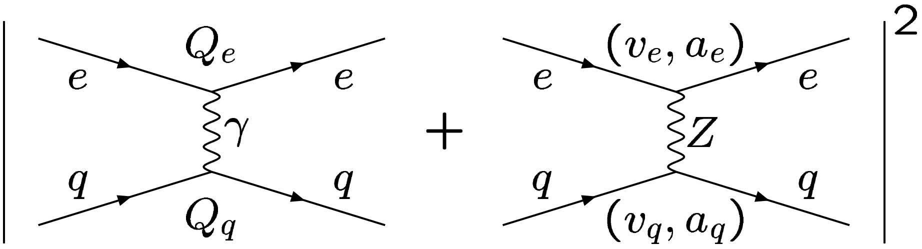


$\sigma(eq \to \nu q') \propto$

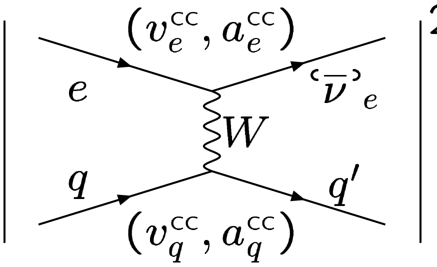


Given by electroweak sector of Standard Model
as functions of $\alpha$, $G_F$, $\sin^2\theta_W$, $(m_t, m_H)$

# DIS Cross–Section Formulae (NC)

$$\boxed{\frac{d^2\sigma^{e^\pm p \to e^\pm X}}{dx\,dQ^2} = \frac{2\pi\alpha^2}{Q^4}\left[Y_+ \cdot \mathcal{F}_2^{\mathrm{NC}} \mp Y_- \cdot \mathcal{F}_3^{\mathrm{NC}}\right]}$$

$$\begin{aligned}
Y_\pm &= \left(1 \pm (1-y)^2\right) \\
\mathcal{F}_2^{\mathrm{NC}} &= \sum_{q=d,u,s,c,b} A_q \cdot [q + \bar{q}] \\
\mathcal{F}_3^{\mathrm{NC}} &= \sum_{q=d,u,s,c,b} B_q \cdot [q - \bar{q}] \\
A_q &= Q_q^2 - 2Q_q v_e v_q \cdot P_Z + (v_e^2 + a_e^2)(v_q^2 + a_q^2) \cdot P_Z^2 \\
B_q &= \qquad - 2Q_q a_e a_q \cdot P_Z + 4 v_e a_e v_q a_q \cdot P_Z^2 \\
P_Z &= \frac{Q^2}{Q^2 + M_Z^2}
\end{aligned}$$

→ Photon–exchange dominates at low $Q^2$

→ For $Q^2 \gtrsim M_Z^2$, $\gamma$ and $Z$ contributions are similar

→ Radiative corrections are substantial.

# DIS Cross–Section Formulae (CC)

$$\frac{d^2\sigma^{e^+p\to\nu X}}{dx\,dQ^2} = \frac{G_F^2}{2\pi} P_W^2 \left[(\bar{u}+\bar{c}) + (1-y)^2(d+s)\right]$$

$$\frac{d^2\sigma^{e^-p\to\bar{\nu} X}}{dx\,dQ^2} = \frac{G_F^2}{2\pi} P_W^2 \left[(u+c) + (1-y)^2(\bar{d}+\bar{s})\right]$$

$$P_W = \frac{M_W^2}{Q^2 + M_W^2}$$

→ $e^+$ and $e^-$ couple to different quark flavors

→ $e^+p$ cross–section dominated by $d$ and $\bar{q}$

→ $y$–dependence useful to disentangle $q$ and $\bar{q}$

→ $b, t$ contributions compressed by $m_t$ and CKMM

→ At low $Q^2$: weak $Q^2$ dependence

→ At high $Q^2$: some sensitivity to $W$ mass

→ Similar formulae for '$\bar{\nu}$'$p$, '$\bar{\nu}$'$N$ scattering

→ Radiative corrections are substantial

# Comparison of NC and CC Cross–Sections

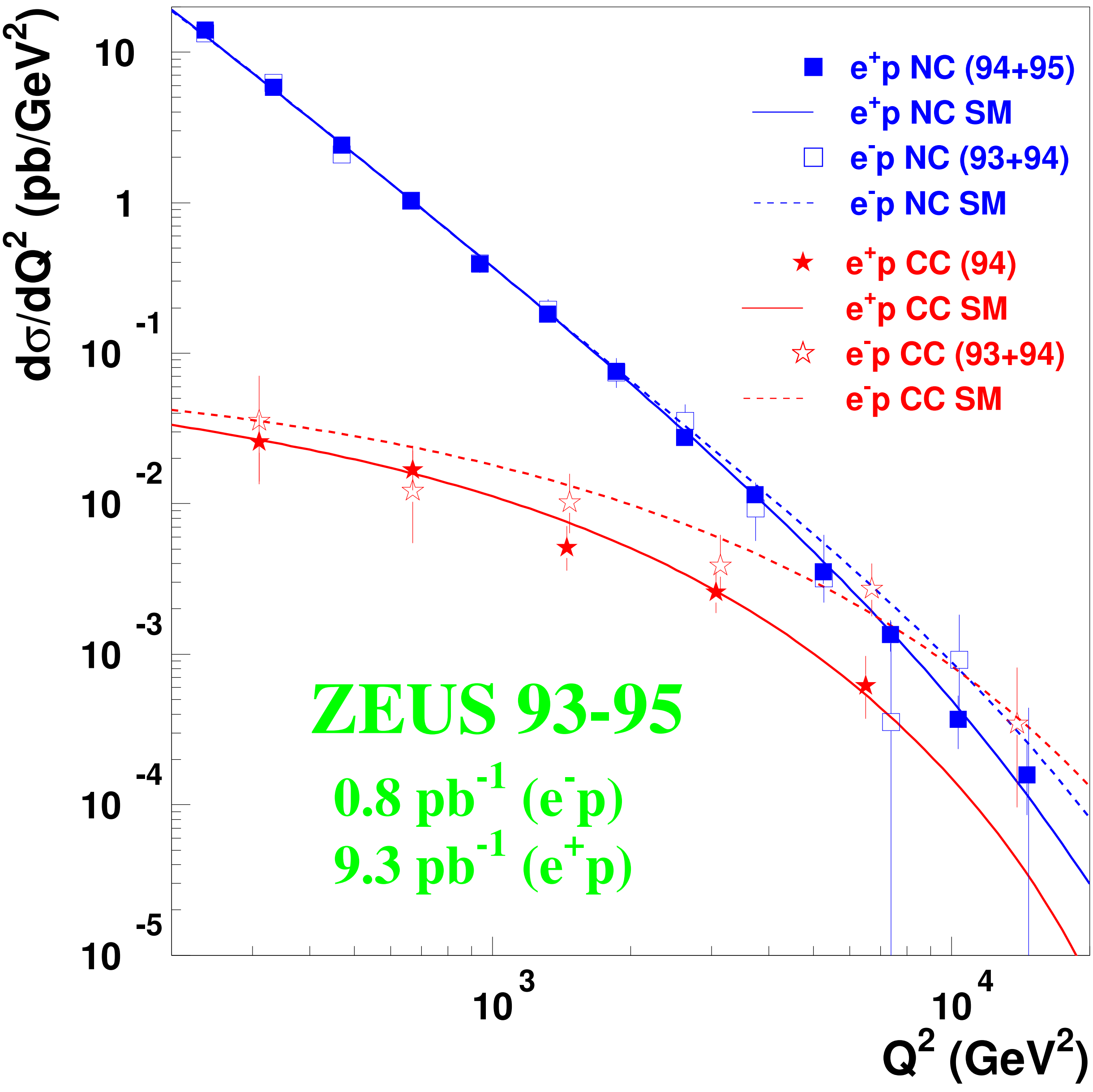


→ At low $Q^2$, $\sigma(\mathrm{CC}) \ll \sigma(\mathrm{NC})$

→ At $Q^2 \gtrsim M_Z^2$, $\sigma(\mathrm{CC}) \sim \sigma(\mathrm{NC})$

1995 data are of very limited precision

# PDF's and QCD

## Leading–order QCD contributions to DIS diagrams:

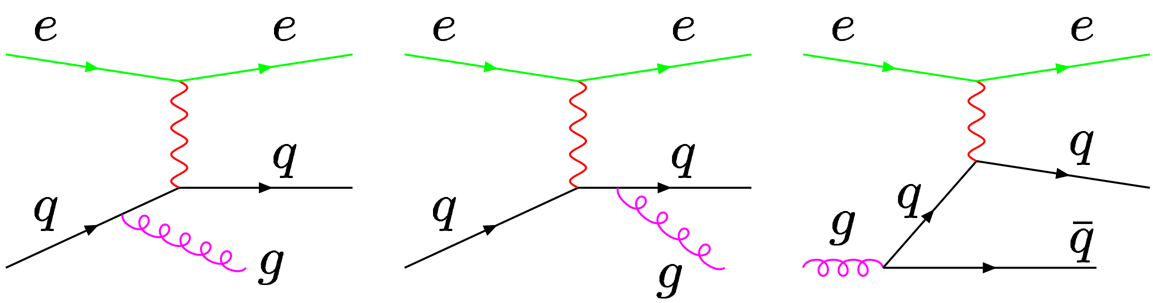


→ Leading modifications are of $\mathcal{O}(\alpha_s \ln Q^2)$

→ Absorbed into effective PDF's

## DGLAP evolution:

(Dokshizer, Gribov, Lipatov, Altarelli, Parisi)

simplified form:

$$\frac{df_{q/p}(x,Q^2)}{d\ln Q^2} = \frac{\alpha_s}{2\pi}\int_x^1 \frac{d\xi}{\xi} f_{q/p}(\xi,Q^2)\,P(\frac{x}{\xi}) + \mathcal{O}({\alpha_s}^2)$$

$P(x/\xi)$ = splitting function (given by QCD)

→ DGLAP evolution fixes $Q^2$ dependence of PDF's

→ PDF's are evolved towards higher $Q^2$ and lower $x$

→ Effectively all terms of $\mathcal{O}({\alpha_s}^n(\ln Q^2)^n)$ are summed

→ Usually employed in next–to–leading order

# PDF Determination

## PDF fitting technique:

→ Parametrise PDF's as function of $x$ for $Q^2 = Q_0^2$

→ Perform QCD evolution

→ Calculate cross–sections, structure functions, etc.

→ Determine parameters by fit to experimental data

- Experimental input data:
  - → $eN$ and $\mu N$ data (HERA, fixed–target)
  - → '$\overline{\nu}$'$N$ data (fixed–target)
  - → $W$ production in $p\bar{p}$ experiments
  - → Drell–Yan lepton–pair production
- Problems:
  - → Low $Q^2$: edge of perturbative QCD regime
  - → Higher–twist terms at low $Q^2$, high $x$
  - → Theoretical treatment of heavy quark PDF's
  - → Higher–order QCD terms (small effect for high $Q^2$)
  - → Nuclear effects in deuteron (may affect $d$ at high $x$)
- Further uncertainties:
  - → Experimental errors on input data (dominant)
  - → Uncertainty of $\alpha_s$
  - → Analytical form of PDF parametrisation
  - → Choice of renormalisation/factorisation scales

# Proton $\mathcal{F}_2$ Structure Function Data

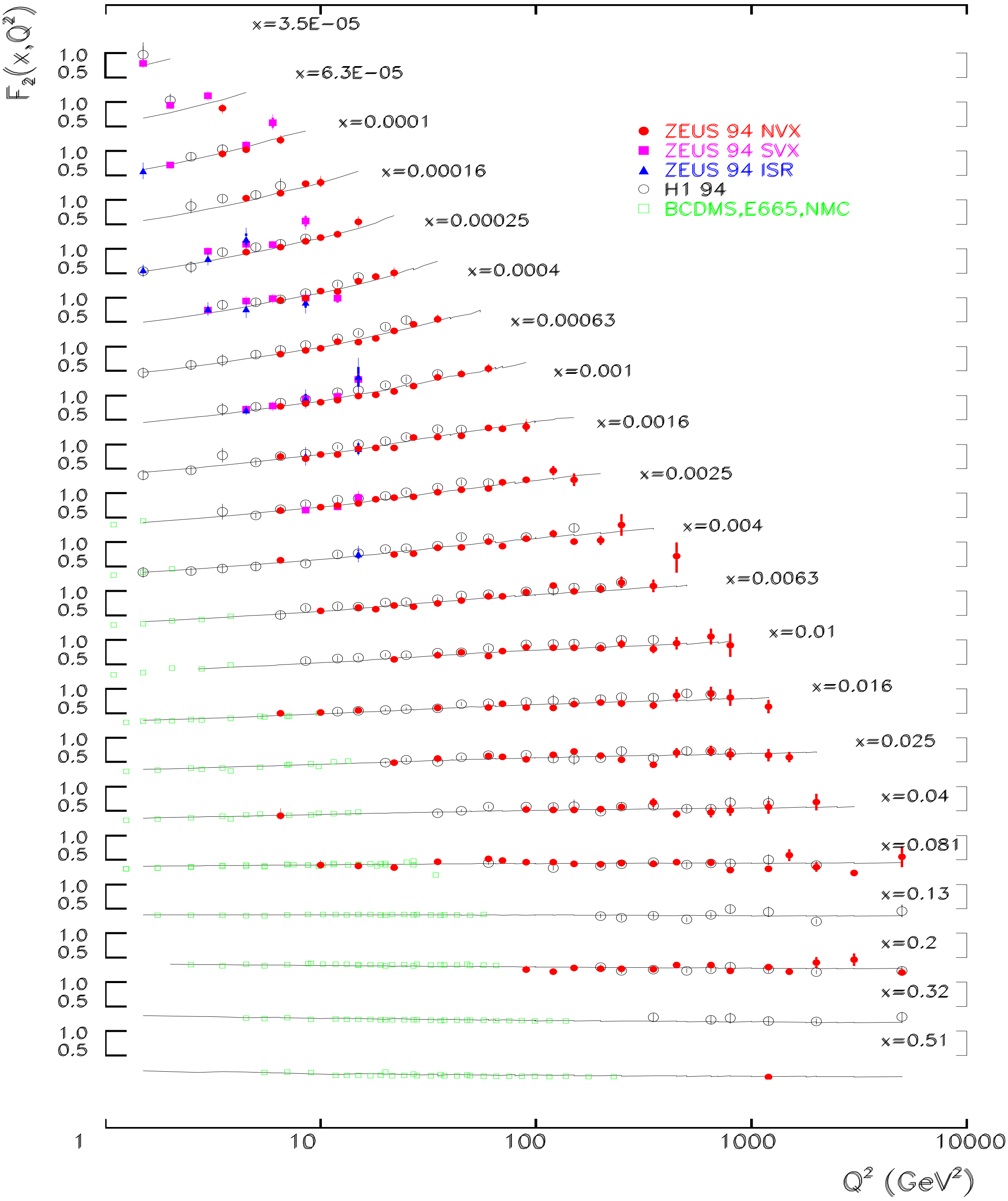


→ Data span several decades in $x$ and $Q^2$

→ QCD fit gives good description

→ Fit at high $x$ driven by fixed–target data

# PDF Uncertainties

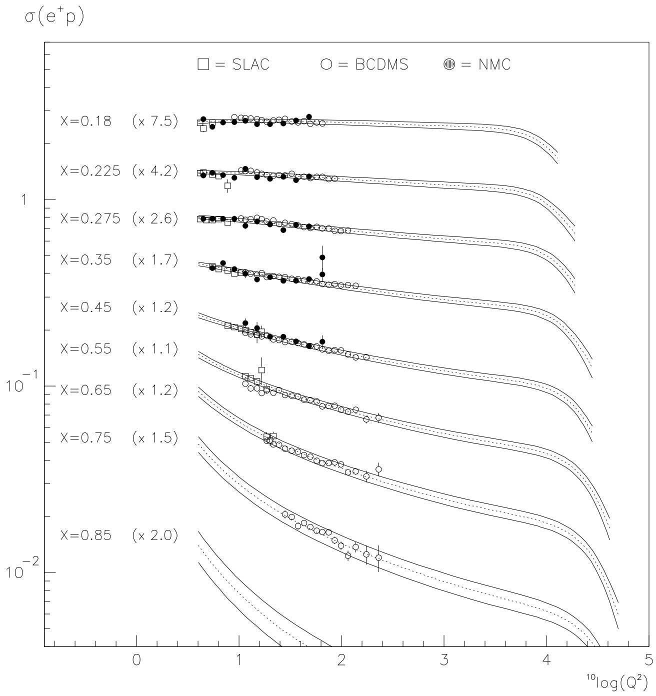


**NC:**

$$\tilde{\sigma} = \frac{xQ^4}{2\pi\alpha^2 Y_+} \frac{d^2\sigma}{dx\,dQ^2}$$

$$\Delta\tilde{\sigma}/\tilde{\sigma} \lesssim 6.5\%$$

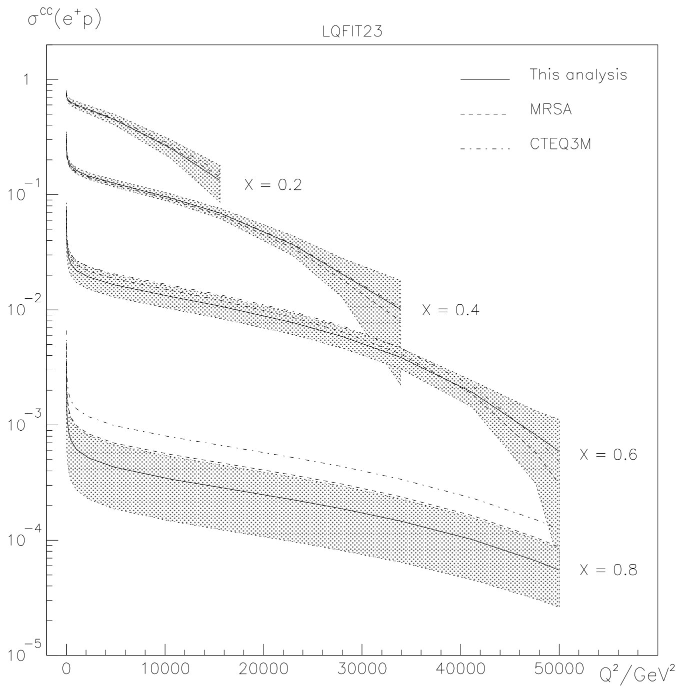


**CC:**

$$\tilde{\sigma} = x \frac{2\pi}{G_F^2 P_W^2} \frac{d^2\sigma}{dx\,dQ^2}$$

$$\Delta\tilde{\sigma}/\tilde{\sigma} \gtrsim 20\%$$

for $x \gtrsim 0.5$ or

$Q^2 \gtrsim 2 \cdot 10^4$ GeV$^2$

→ $\tilde{\sigma}$ = reduced cross–section (∼PDF's)

→ Experimental errors on input data and on $\alpha_s$ were propagated in QCD fit (M. Botje, ZEUS)

# PDF's in the High–$Q^2$ Regime

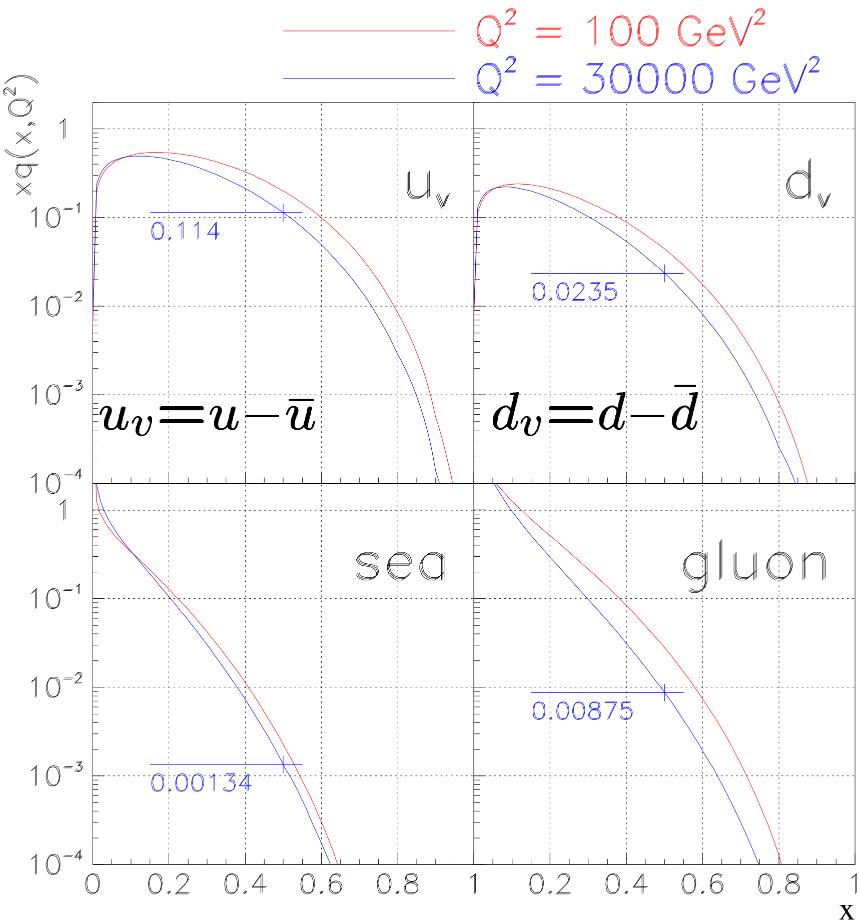


- → For $x \gtrsim 0.2$ valence $\gg$ sea
- → $d/u \ll 0.5$ for $x \to 1$
- → $\sigma^{e^\pm p}$(NC) is dominated by $u$
- → $\sigma^{e^+ p}$(CC) is dominated by $d$

## QCD evolution and spatial resolution:

- → Spatial resolution improves with $Q^2$
- → $e$ "sees" more partons having lower momentum
- → Valence distributions are reduced

## Non–Standard PDF Scenarios

- Modified gluon density (CDF jets):
  - → DIS dominated by $eq$ processes
  - → Gluon modification has small effect in DIS
- Intrinsic charm:
  - → Model: $\mathcal{O}(1\%)$ of the proton momentum is carried by valence–like $c/\bar{c}$ quarks
  - → Modifies cross–section at high $x$
  - → Effect larger in CC than in NC
- The $d/u$ ratio::
  - → All current PDF's use $d/u \to 0$ at $x \to 1$
  - → Consistent relativistic treatment of deuteron data indicates that this may be wrong
    Melnitchouk, Thomas, Phys.Lett.B377(96)11
  - → Possible increase of $d$ at large $x$
  - → Mainly affects $e^+p$ CC cross–section

- All modifications at large $x$ ($\gtrsim$ 0.4)
- Larger effects in CC than in NC
- No explanation for large high–$Q^2$ excess

# Cross–Section Measurements

→ 1994–1996 data:
Excess at high $x$, $Q^2$

→ LP97: Updated results

What we have now:

→ Increased data samples

→ Improved analysis methods

→ Differential cross–sections

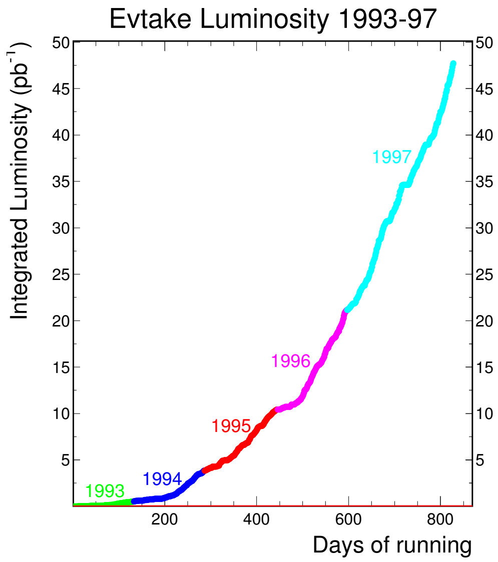


- NC analyses:
  - → Event distributions in $(x, y)$ (ZEUS,H1)
  - → $d\sigma/dQ^2$ (ZEUS,H1), $d\sigma/dx$ (H1)
  - → $d^2\sigma/(dx\,dQ^2)$ and QCD fit (H1)

- CC analyses:
  - → $d\sigma/dQ^2$ (ZEUS,H1)
  - → reduced cross–section (H1)

Focus on results
Only few analysis details

# NC Analyses

- Kinematic Reconstruction
  - → 4 independent measurements per event:

    $\theta_e, E'$ (e) $\gamma_h, E_{\text{had}}$ (hadrons)

  - → Only two independent variables ($Q^2 = xys$)
  - → Different reconstruction methods
  - → ZEUS: "double–angle"; H1: $e\Sigma$ ($e$ based)

**Initial State Radiation (ISR):**

- → Photon radiation in $e$ beam direction
- → Photon can escape undetected
- → Effectively reduces $s$
- → $\langle|\Delta_{\text{ISR}} x/x|\rangle, \langle|\Delta_{\text{ISR}} Q^2/Q^2|\rangle = \mathcal{O}(1-3\%)$
- → Shift in opposite directions for ZEUS,H1

- Event Selection:
  - → Require identified scattered electron
  - → Vertex reconstructed and in fiducial region
  - → $E - p_z > 40$ GeV (ZEUS); 35 GeV (H1)

**The $E - p_z$ cut:**

- → $(E - p_z)(\text{final}) = (E - p_z)(\text{initial}) = 2E_e$
- → Cut removes photoproduction and hard ISR

# $Q^2$ Resolution for NC Events (ZEUS)

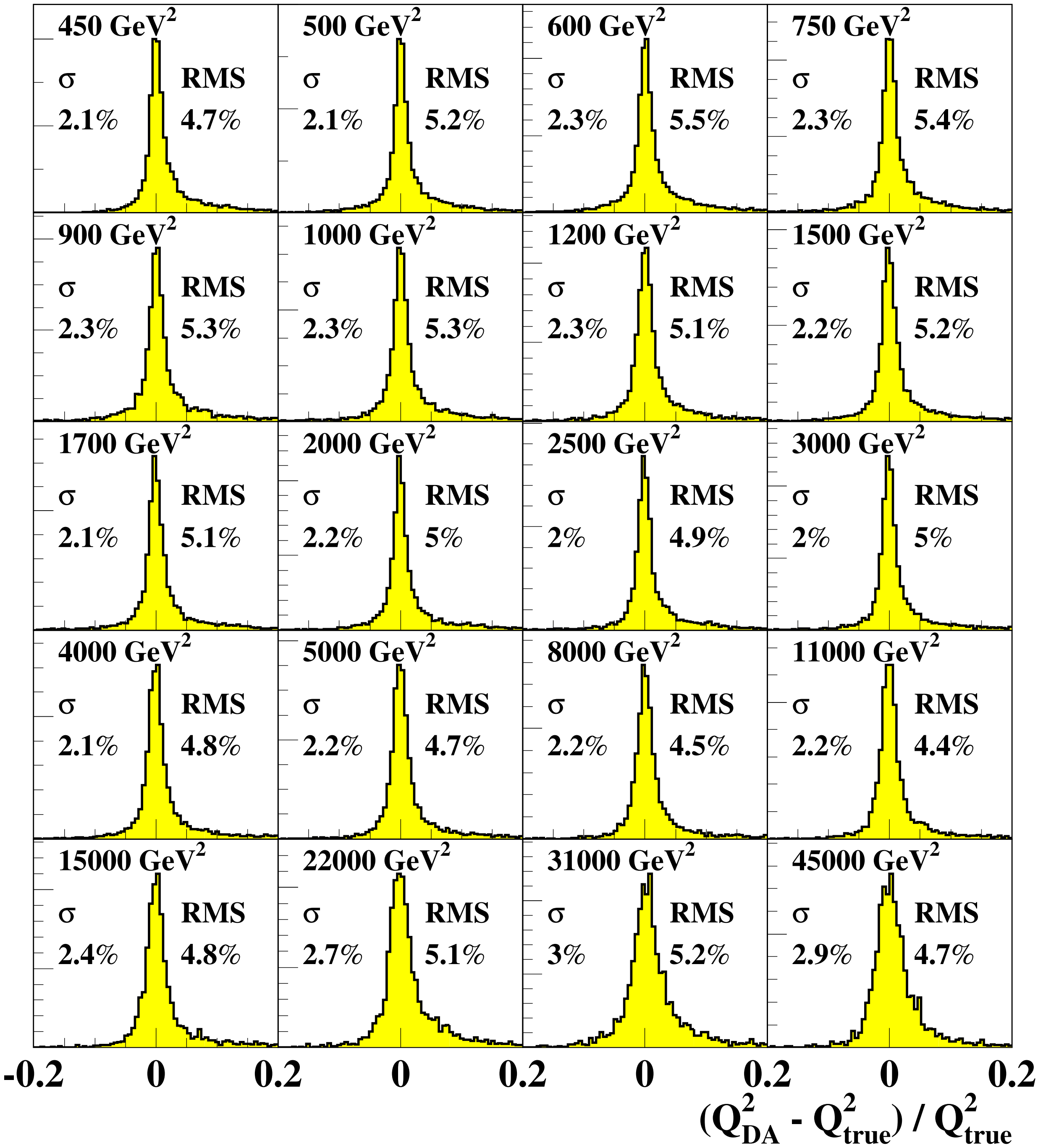


→ Resolution $\Delta Q^2/Q^2$ stable in entire $Q^2$ range

→ Typically $\Delta Q^2/Q^2 = 2-3\%$ (Gaussian width)

# In situ $E'$ Calibration (H1)

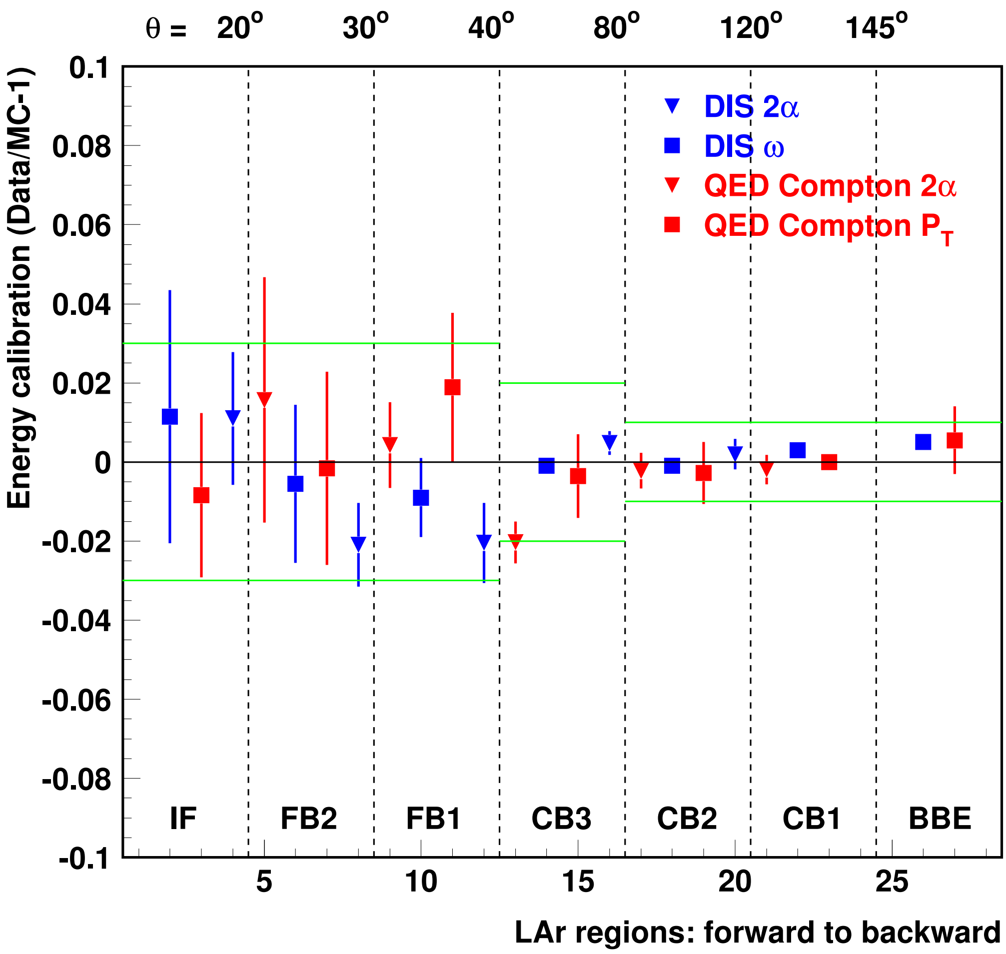


→ Basic method: Use redundancy of NC DIS kinematics to calibrate $E'$

→ Double–angle method yields $E'$ independent of calorimeter energy scale

→ Accuracy still statistics–limited

→ $E'$ energy scale reliable to $1 - 3\%$

→ Similar methods are used by ZEUS

# NC Data Samples and Systematics

## Event Samples:

| ZEUS | H1 |
|---|---|
| $Q^2 > 400\,\mathrm{GeV}^2$ <br> $y_e < 0.95$ | $Q^2 > 200\,\mathrm{GeV}^2$ <br> $y_e < 0.9$ |
| $\sim$ 38000 events | $\sim$ 75000 events |

## Main Systematic Effects:

- Electron energy scale (affects mainly H1)
- Electron finding efficiency
- Accuracy of detector simulation
- Vertex reconstruction
- Trigger efficiency (small effect for ZEUS)
- Luminosity uncertainty ($\sim 2.5\%$)
- Photoproduction background ($< 1\%$)

$\rightarrow$ No dominating source
$\rightarrow$ Typical systematic errors = a few %
$\rightarrow$ Analyses are statistics–limited
for $Q^2$ above a few $1000\,\mathrm{GeV}^2$

# ZEUS Kinematic Plane (NC)

Changes w.r.t. the 1996/LP97 analyses:

Improved analysis algorithms

Slightly modified event selection

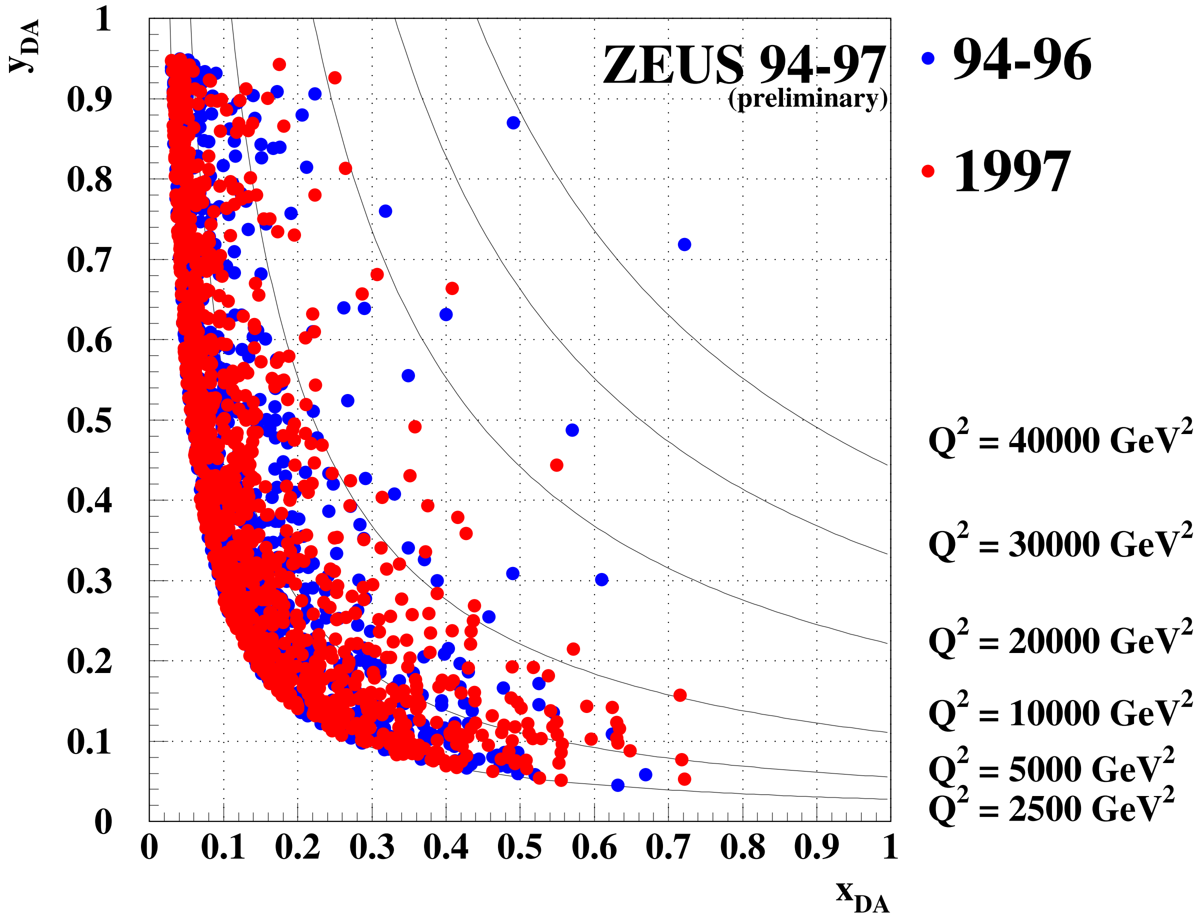


| $Q^2_{\text{min}}$ (GeV$^2$) | $N_{obs}$ | $N_{exp}$ |
|---|---|---|
| 2500 | 1817 | 1792 $\pm$ 93 |
| 5000 | 440 | 396 $\pm$ 24 |
| 10000 | 66 | 60 $\pm$ 4 |
| 15000 | 20 | 17 $\pm$ 2 |
| 35000 | 2 | 0.29 $\pm$ 0.02 |

# H1 Kinematic Plane (NC)

Changes w.r.t. the 1996/LP97 analyses:

New $E'$ calibration

Slightly modified event selection

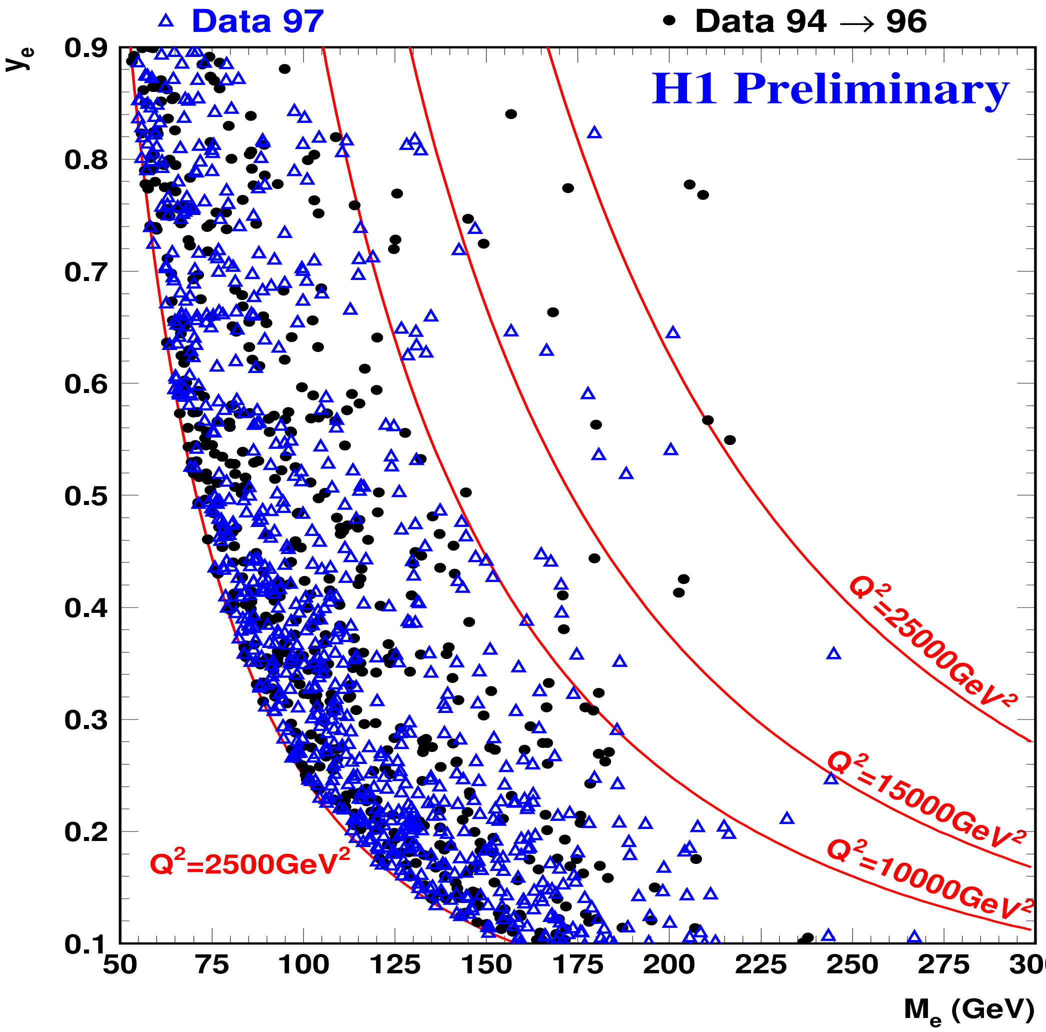


| kinematic region | $N_{obs}$ | $N_{exp}$ |
|---|---|---|
| $Q^2 > 15000$ GeV$^2$ | 22 | 14.7 $\pm$ 2.1 |
| $M_e = (200 \pm 12.5)$ GeV | 8 | 3.01 $\pm$ 0.54 |
| (94–96) | 7 | 0.95 $\pm$ 0.18 |

# NC Cross–Section Status at LP97

ZEUS and H1 NC 1994–1997, LP97

(based on about 70% of the current data samples)

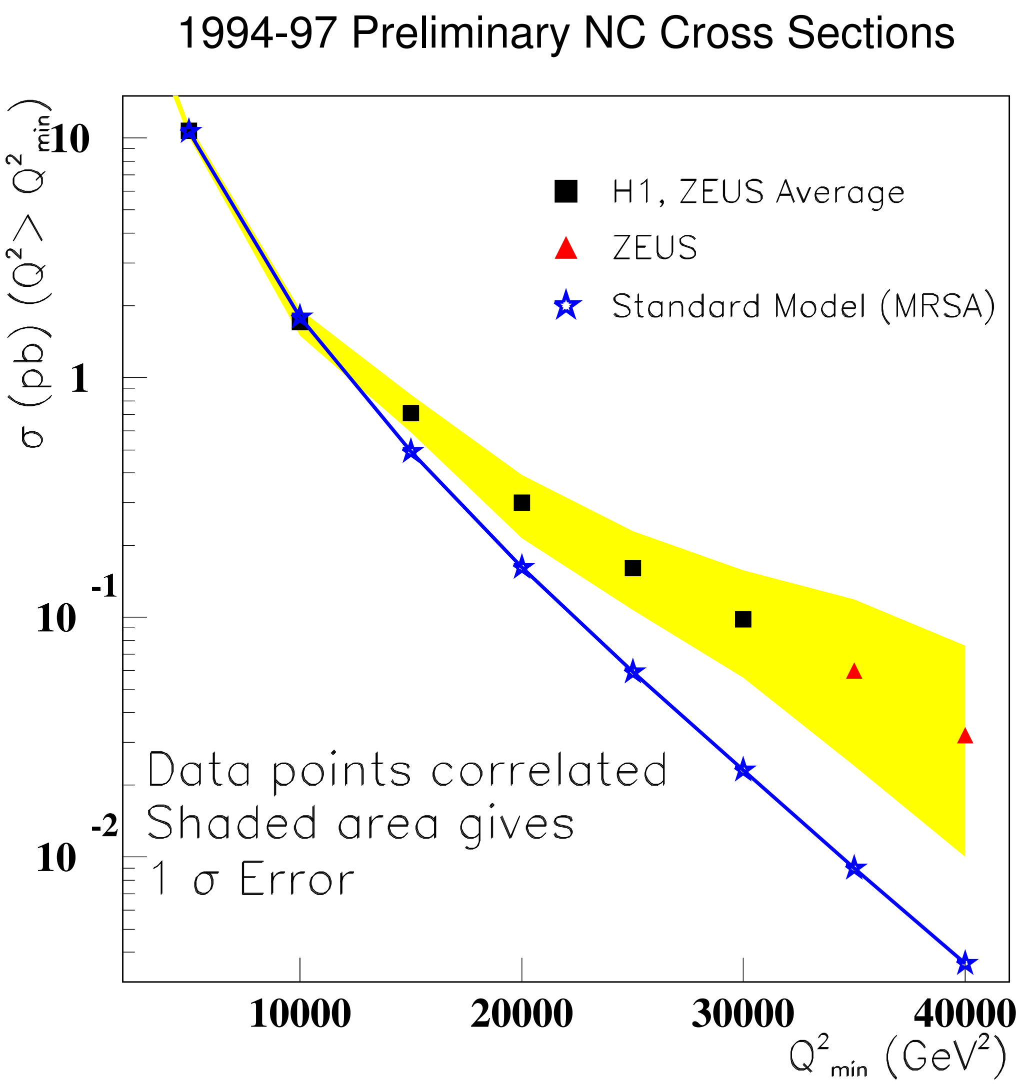


- → Indication of cross–section excess
- → Deviation data – SM increases with $Q^2$
- → Let's look at $d\sigma/dQ^2$ first

# NC Cross–Section $d\sigma/dQ^2$ (ZEUS)

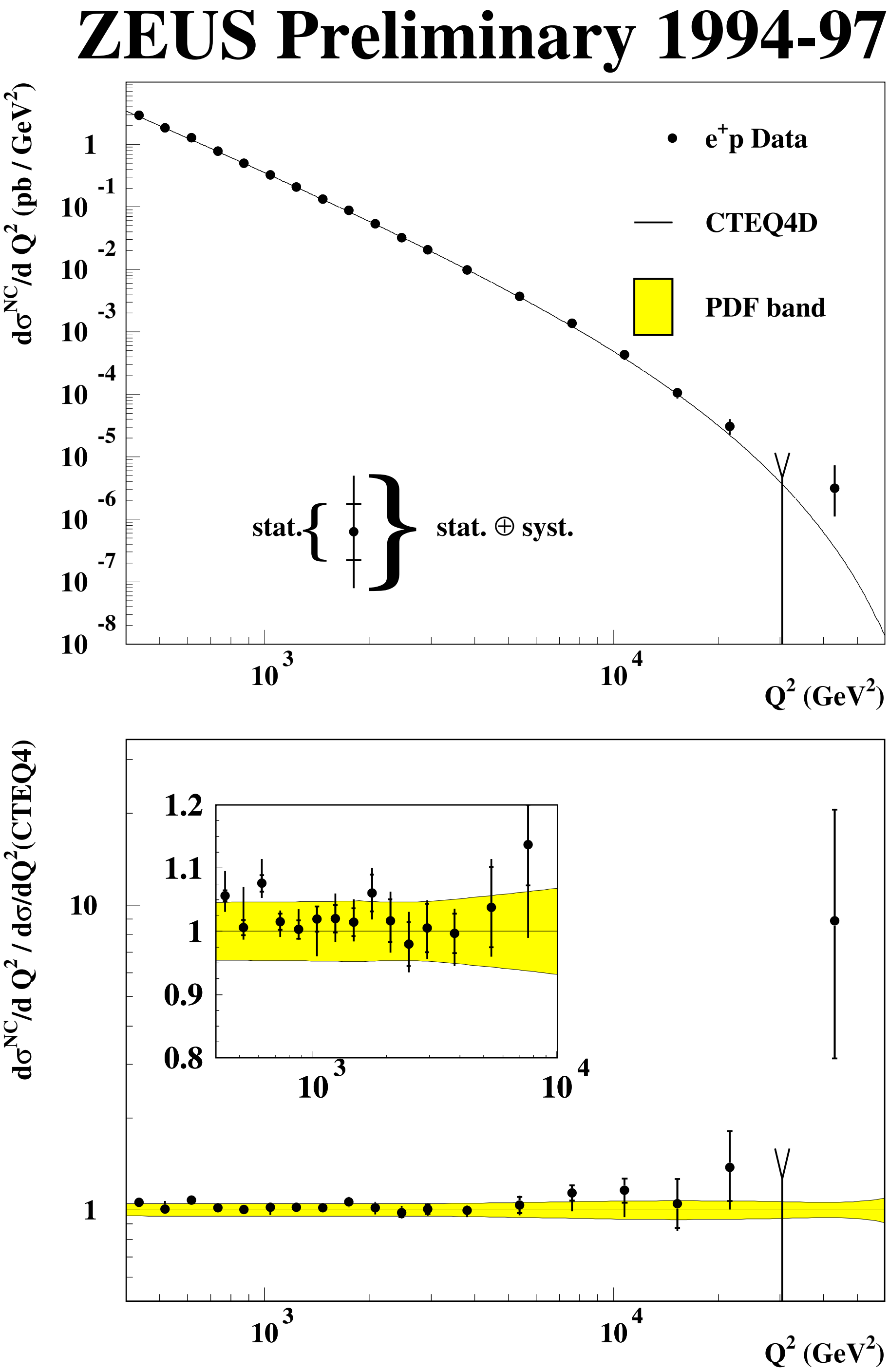


- → Error band = PDF uncertainty
- → Very good agreement with SM prediction
- → Slight excess at highest $Q^2$

# NC Cross–Section $d\sigma/dQ^2$ (H1)

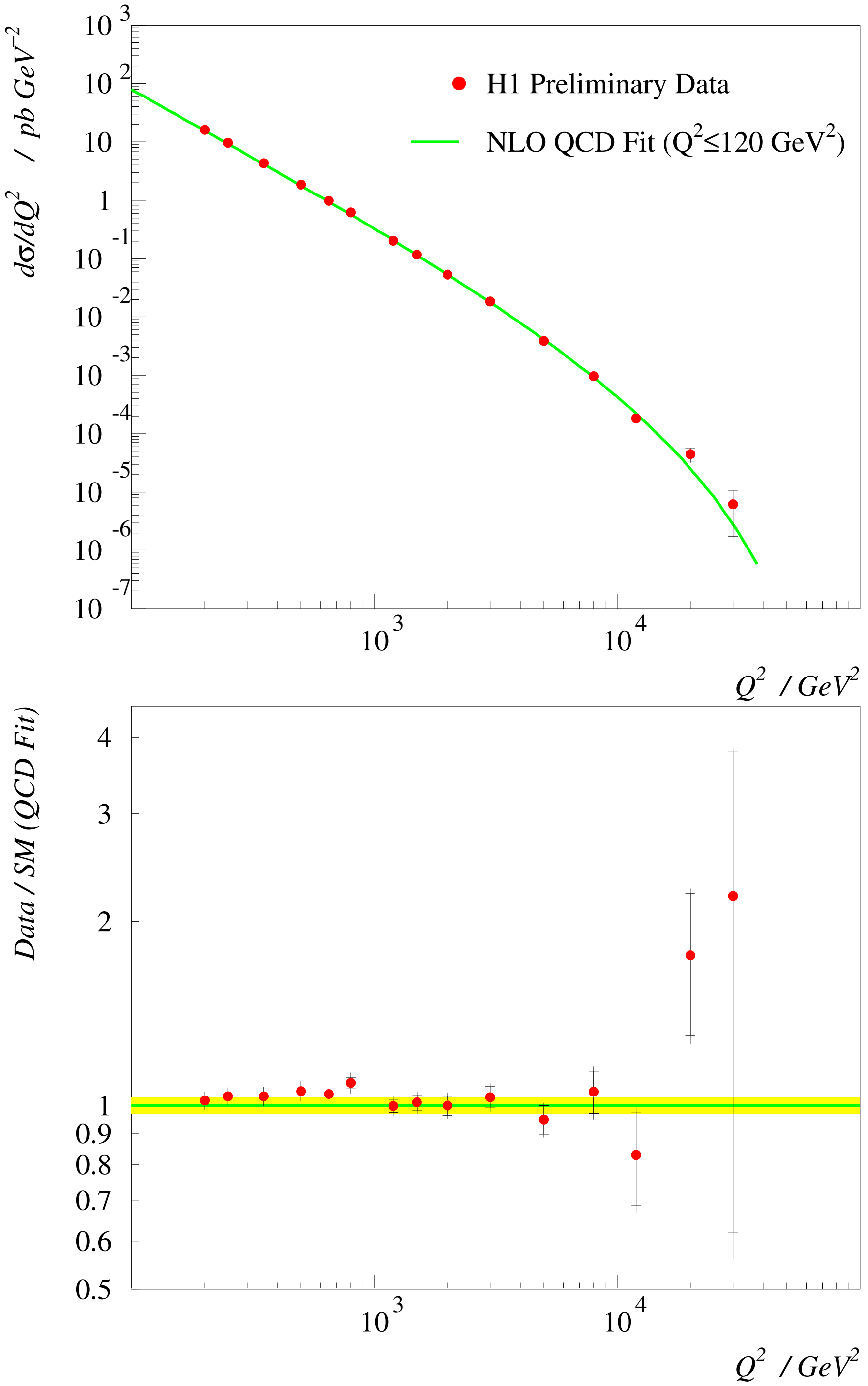


→ Error band = luminosity uncertainty

→ Very good agreement with SM prediction

→ Slight excess at highest $Q^2$

# NC Cross–Section $d\sigma/dx$ (H1)

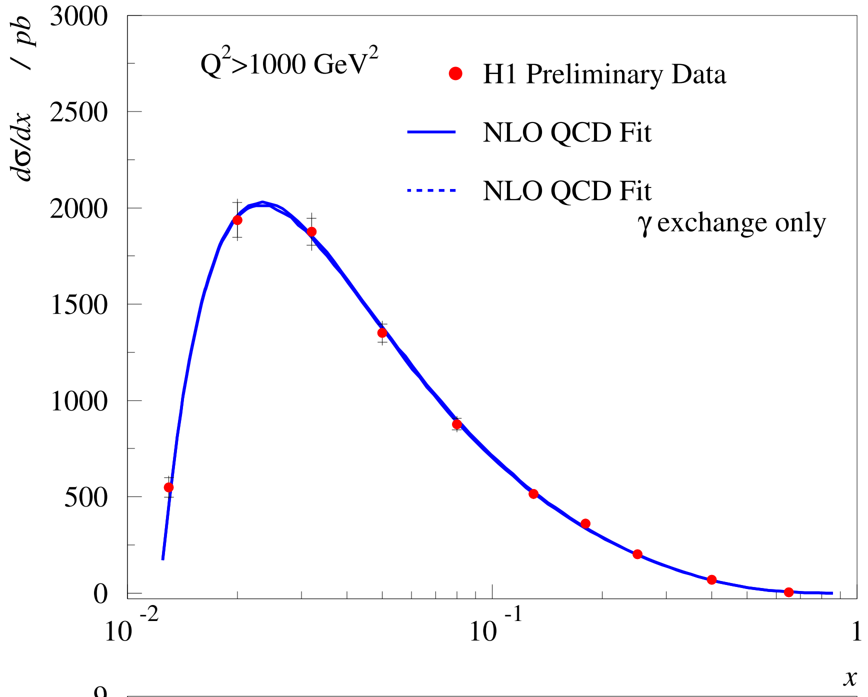


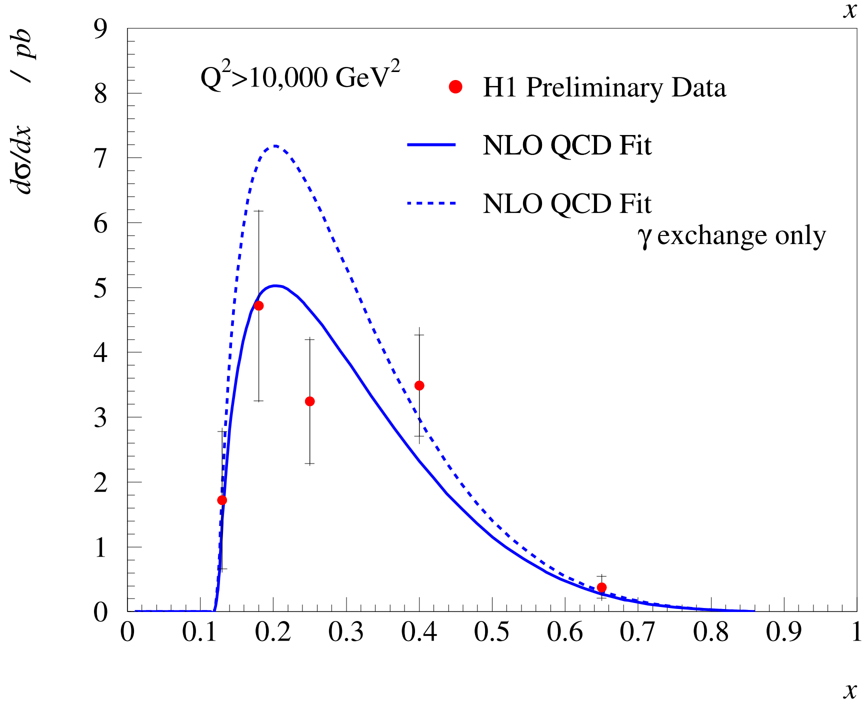


→ No indication of excess at highest $x$

→ Some sensitivity to electroweak effects

→ Good agreement with SM prediction

# Reduced NC Cross–Section (H1)

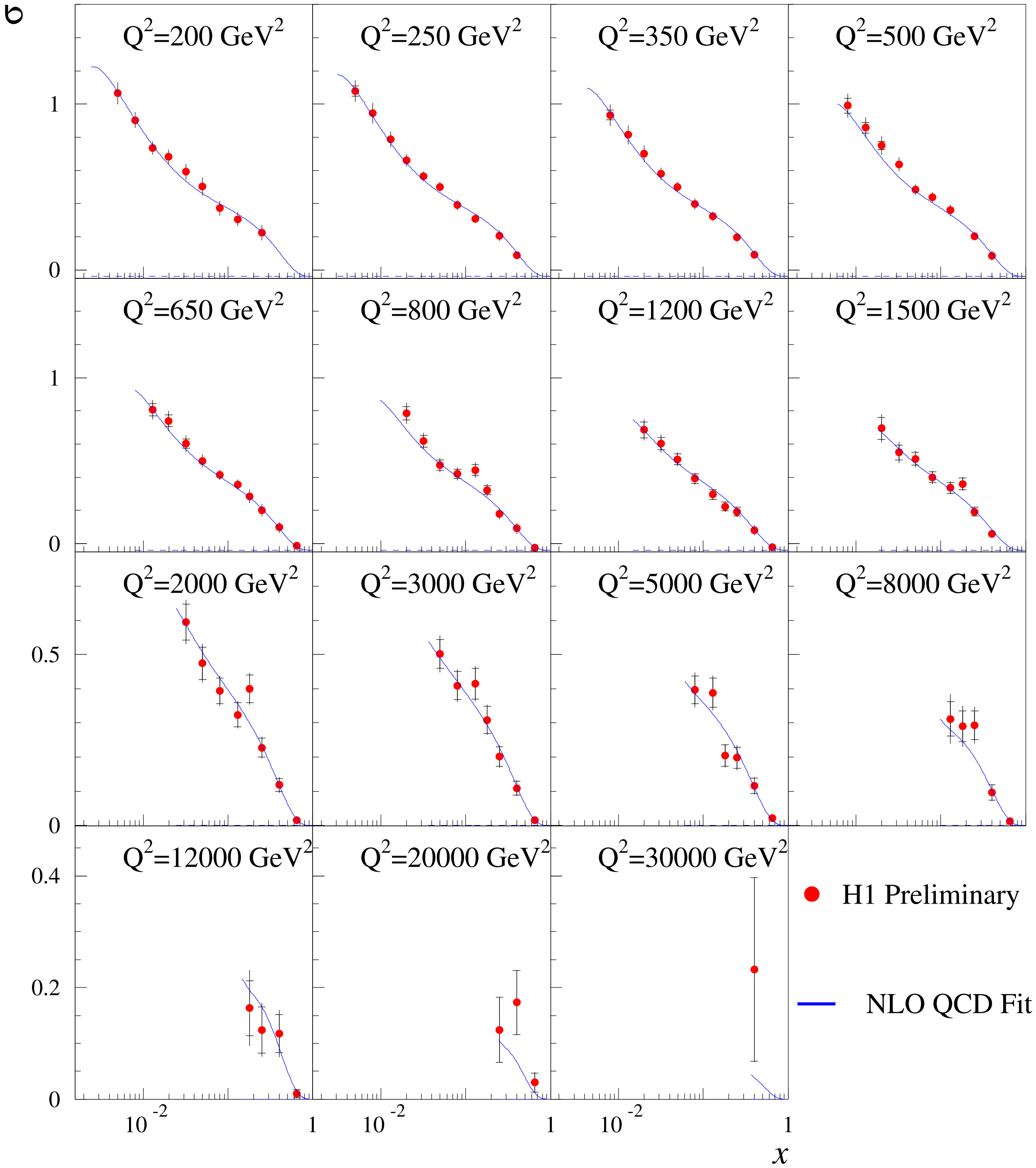


→ Measurements cover region
$x < 0.65$ and $Q^2 < 30000\,\mathrm{GeV}^2$

→ QCD fit to lower–$Q^2$ data describes $\tilde{\sigma}$ in complete $(x, Q^2)$ range

→ Highest–$Q^2$ bins suffer from low statistics

# Reduced NC Cross–Section (H1) contd.

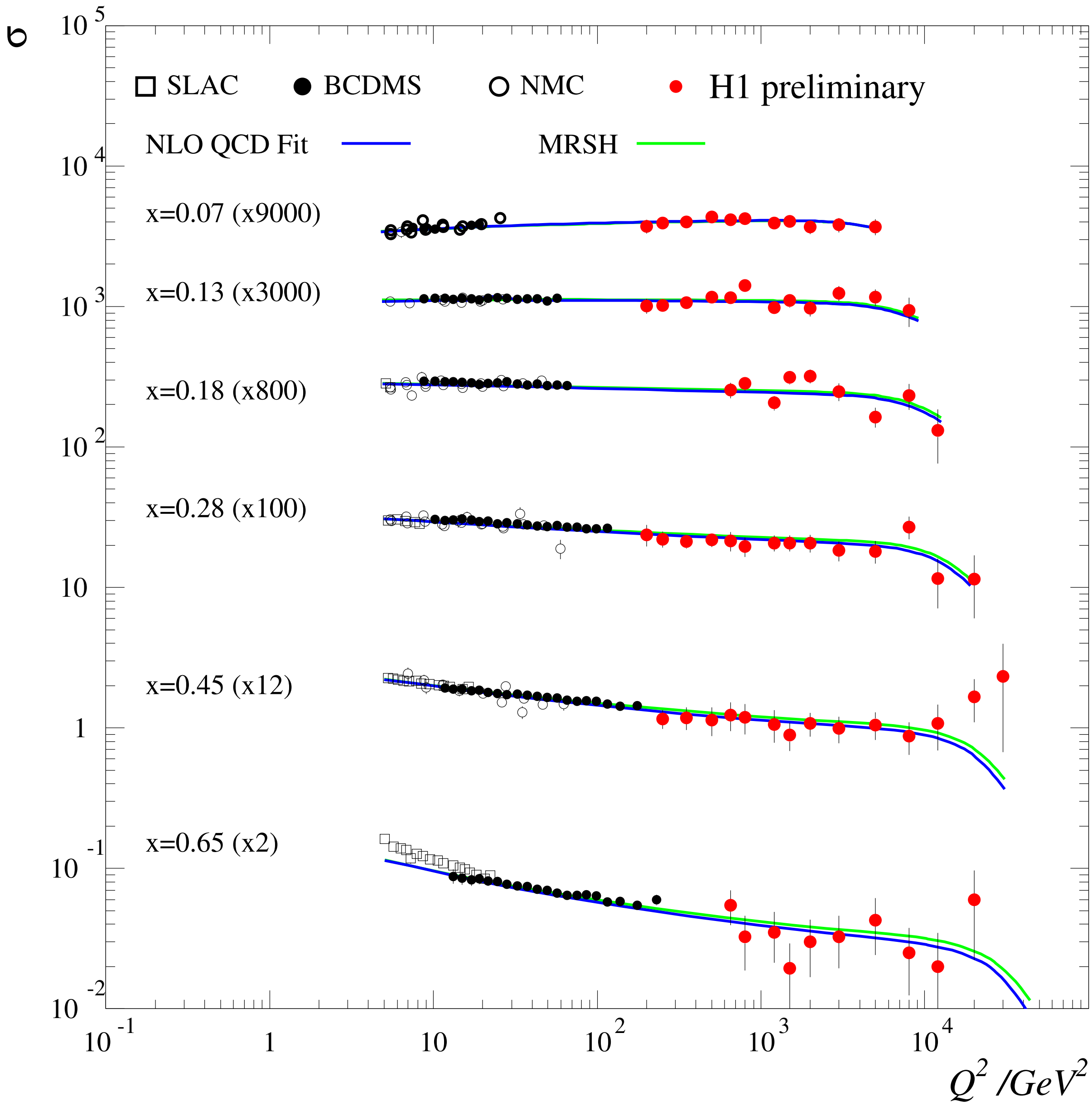


- → Gap to fixed–target experiments almost filled
- → No discrepancies HERA/fixed–target obvious
- → Statistical precision still limited
- → Excess at $x \approx 0.45$ remains visible

# CC Analyses

- Kinematic Reconstruction
  - → Scattered neutrino invisible
  - → Use $\gamma_h$ and $E_{\mathrm{had}}$ for reconstruction
- Event Selection:
  - → Main signature: missing $p_t$
    $p_t > 10$ GeV (ZEUS); $p_t > 12$ GeV (H1)
  - → Vertex reconstructed and in fiducial region
  - → Anti–background event topology cuts
- Event Samples:

| ZEUS | H1 |
|---|---|
| $Q^2 > 400\,\mathrm{GeV}^2$<br>$y < 0.9$ | $x > 0.01$<br>$0.03 < y < 0.9$ |
| 869 events | 656 events |

- Systematic Effects:
  - → Dominated by hadronic energy scale

## $Q^2$ Resolution for CC Events (ZEUS)

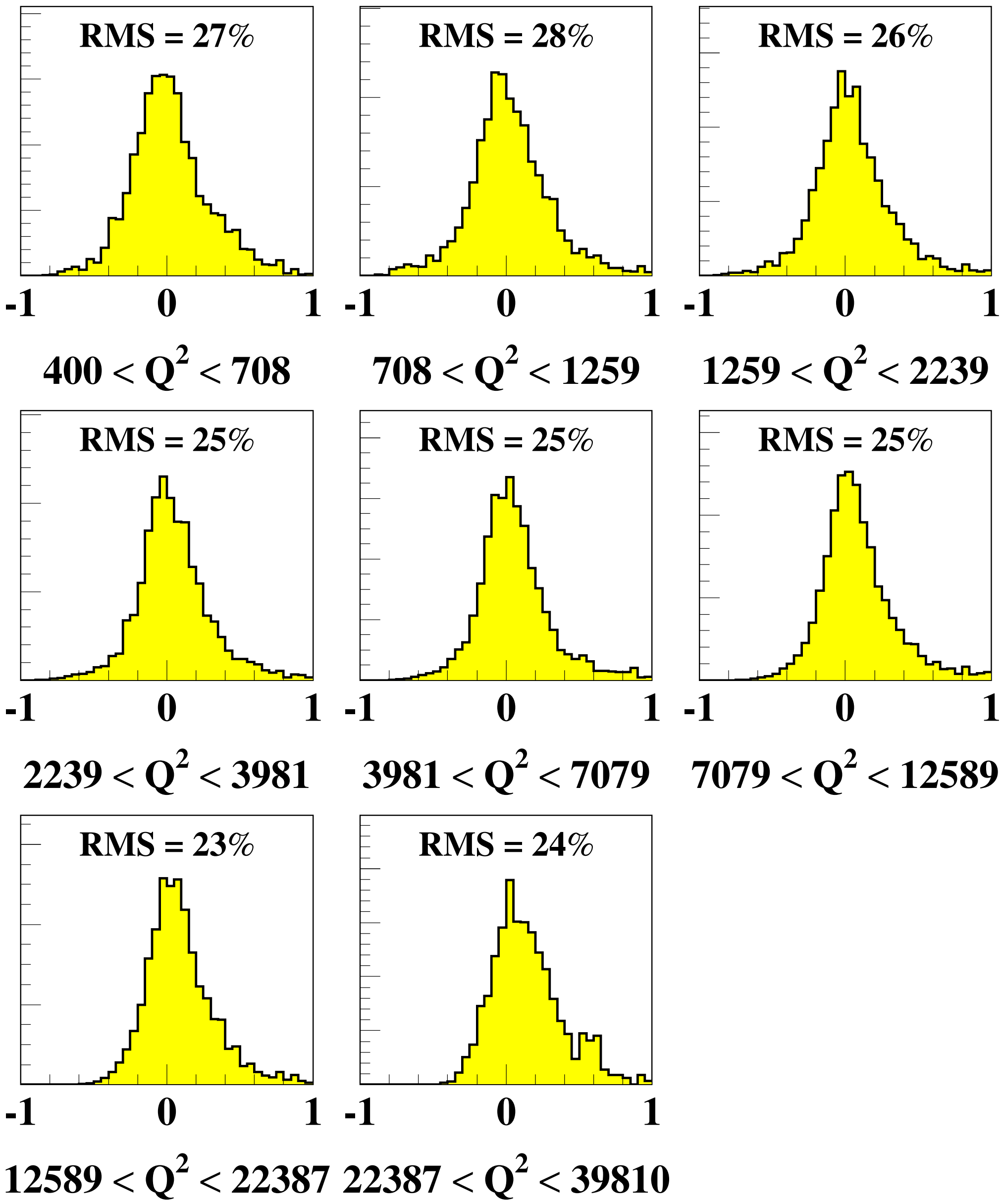


→ Resolution $\Delta Q^2/Q^2$ stable in entire $Q^2$ range

→ Typically $\Delta Q^2/Q^2 \approx 25\%$ (R.M.S.)

# ZEUS Kinematic Plane (CC)

Changes w.r.t. the 1996/LP97 analyses:

Improved analysis algorithms

Modified event selection

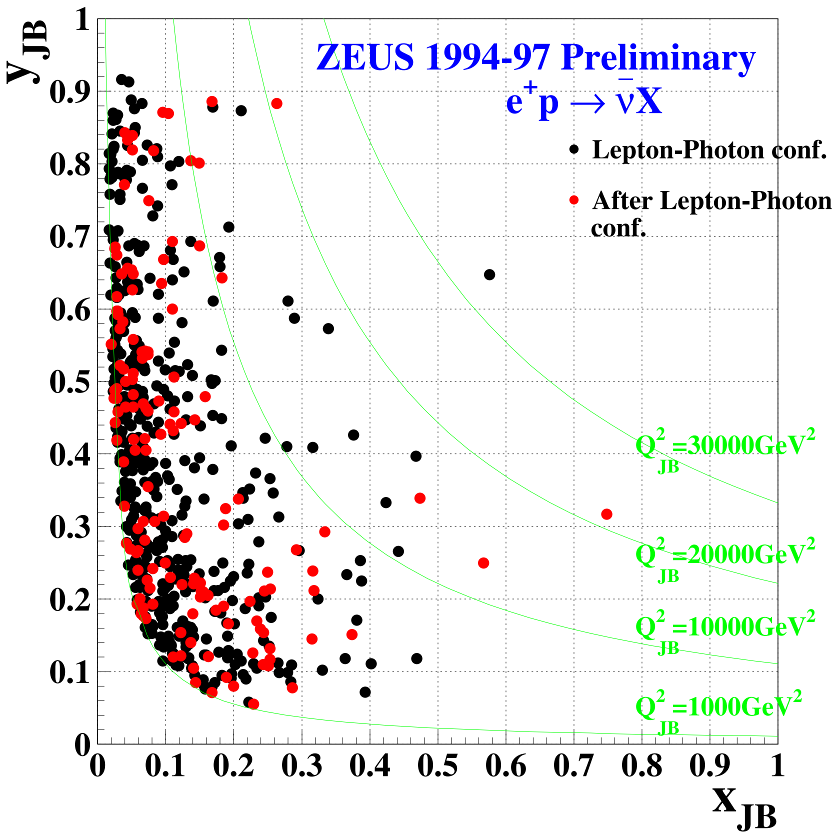


| $Q^2_{\text{min}}$ ( GeV$^2$) | $N_{obs}$ | $N_{exp}$ and errors | | |
|---|---|---|---|---|
| 1000 | 586 | 600 | +52 | -52 |
| 10000 | 22 | 17 | +5.7 | -5.2 |
| 15000 | 8 | 3.9 | +1.9 | -1.6 |
| 20000 | 3 | 0.97 | +0.65 | -0.47 |
| 30000 | 1 | 0.06 | +0.08 | -0.04 |

# CC Cross–Section $d\sigma/dQ^2$ (ZEUS)

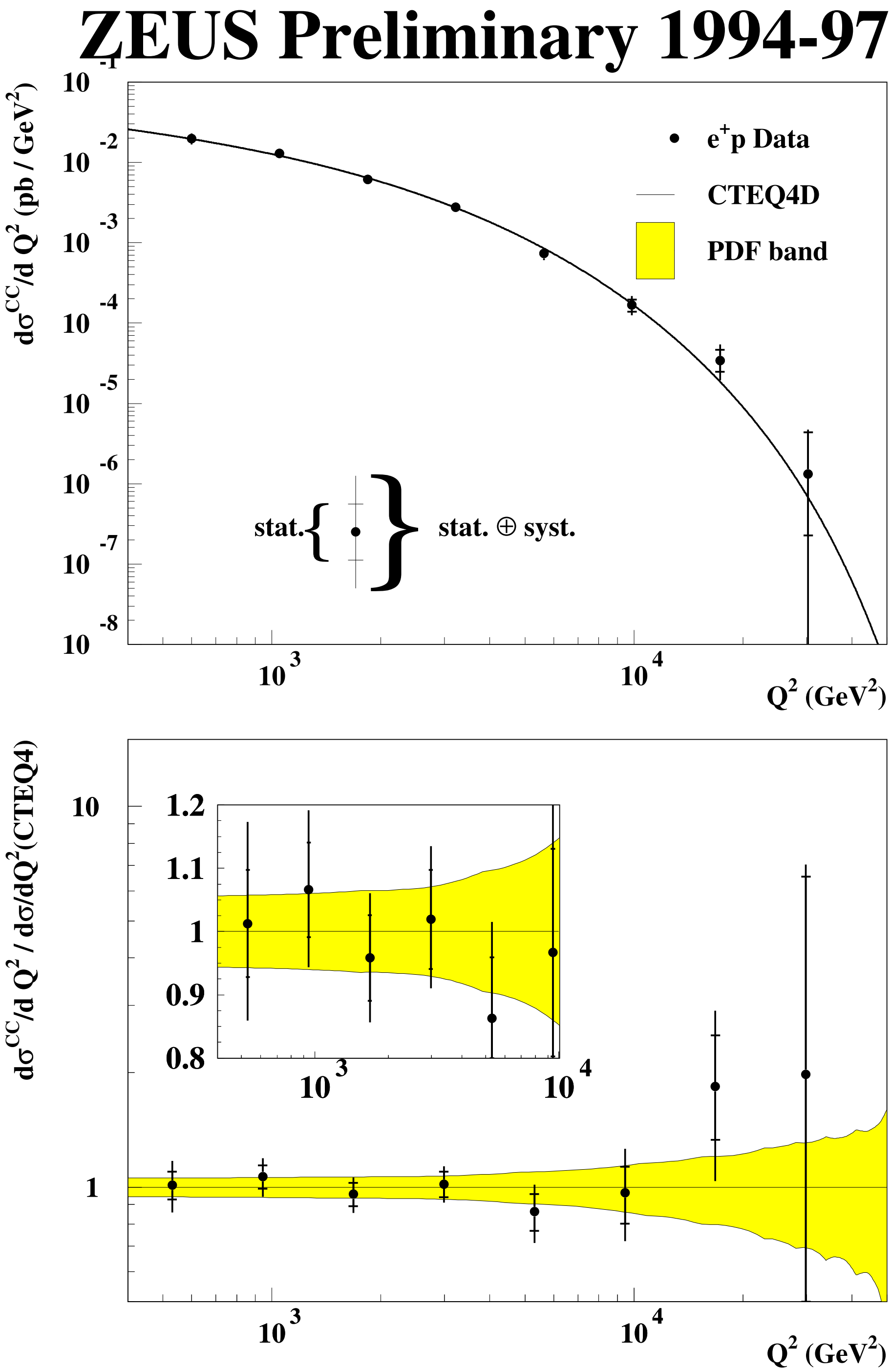


- $\rightarrow$ Error band = PDF uncertainty
- $\rightarrow$ Good agreement with SM prediction
- $\rightarrow$ Slight excess at highest $Q^2$ ?

# CC Cross–Section $d\sigma/dQ^2$ (H1)

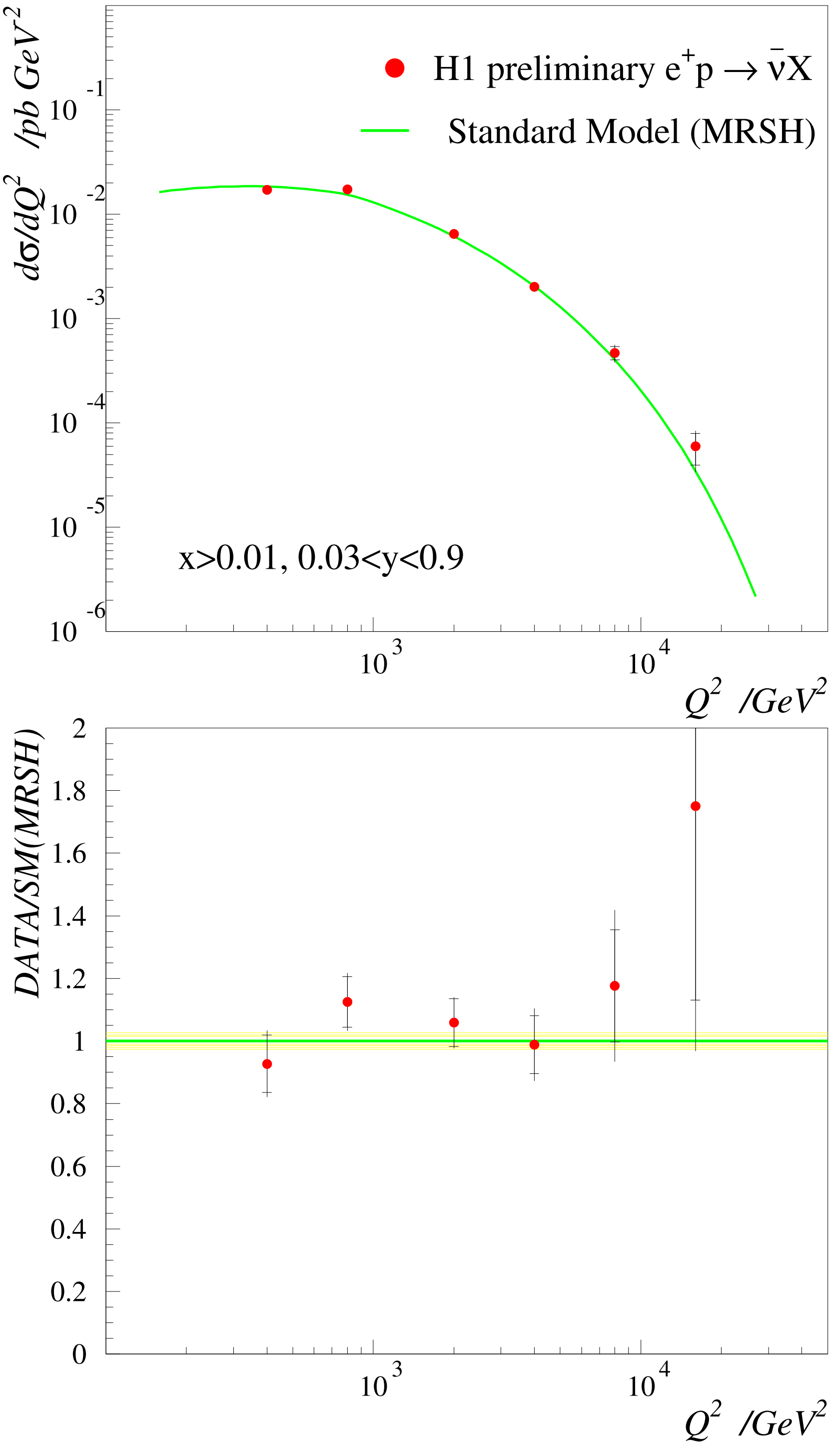


- → Error band = luninosity uncertainty
- → Good agreement with SM prediction
- → Slight excess at highest $Q^2$ ?

# Reduced CC Cross–Section (H1)

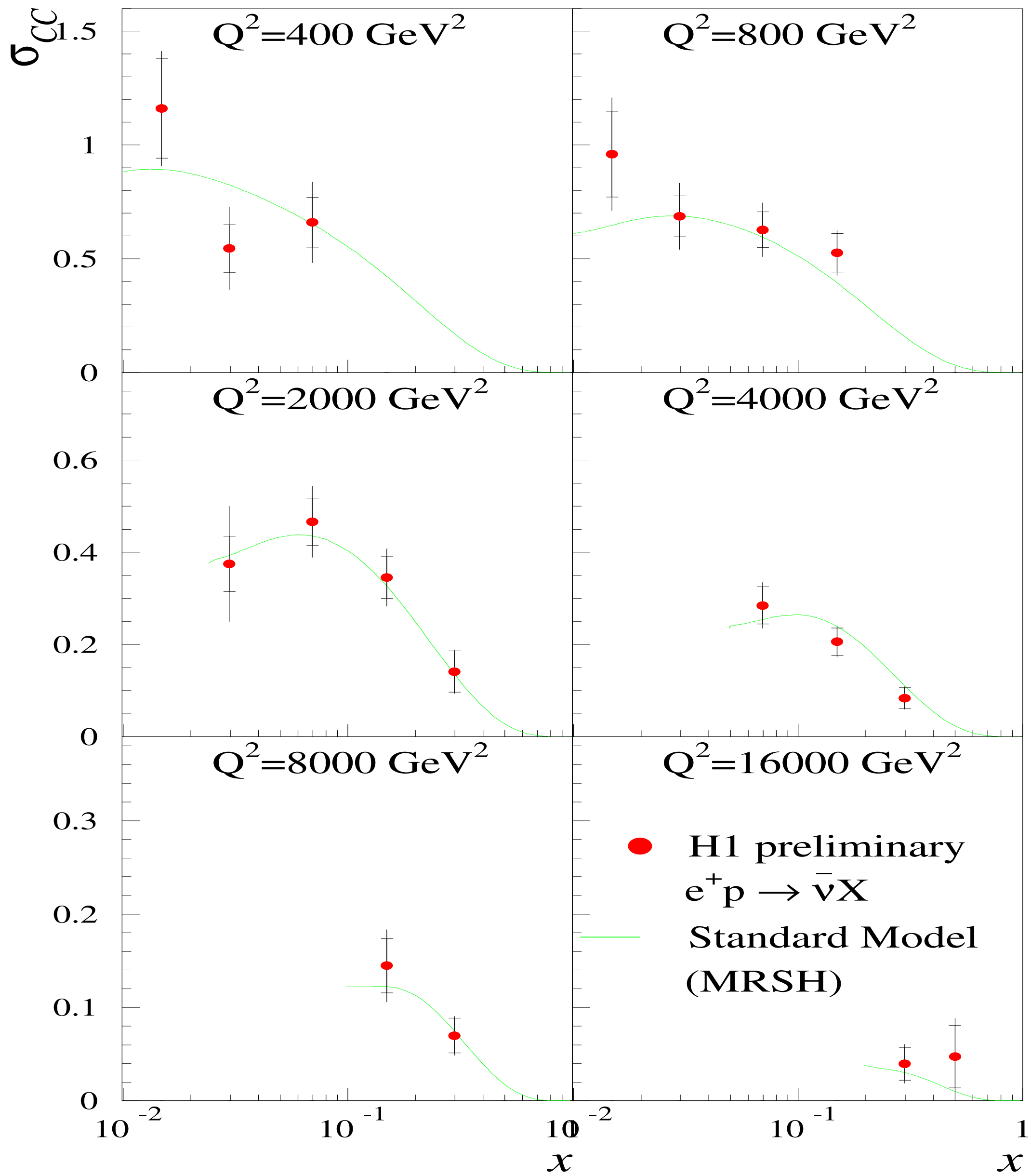


→ Good agreement with SM prediction

→ Data do not yet allow precise study of high–$x$ region ($x \gtrsim 0.3$)

# Reduced CC Cross–Section (contd.)

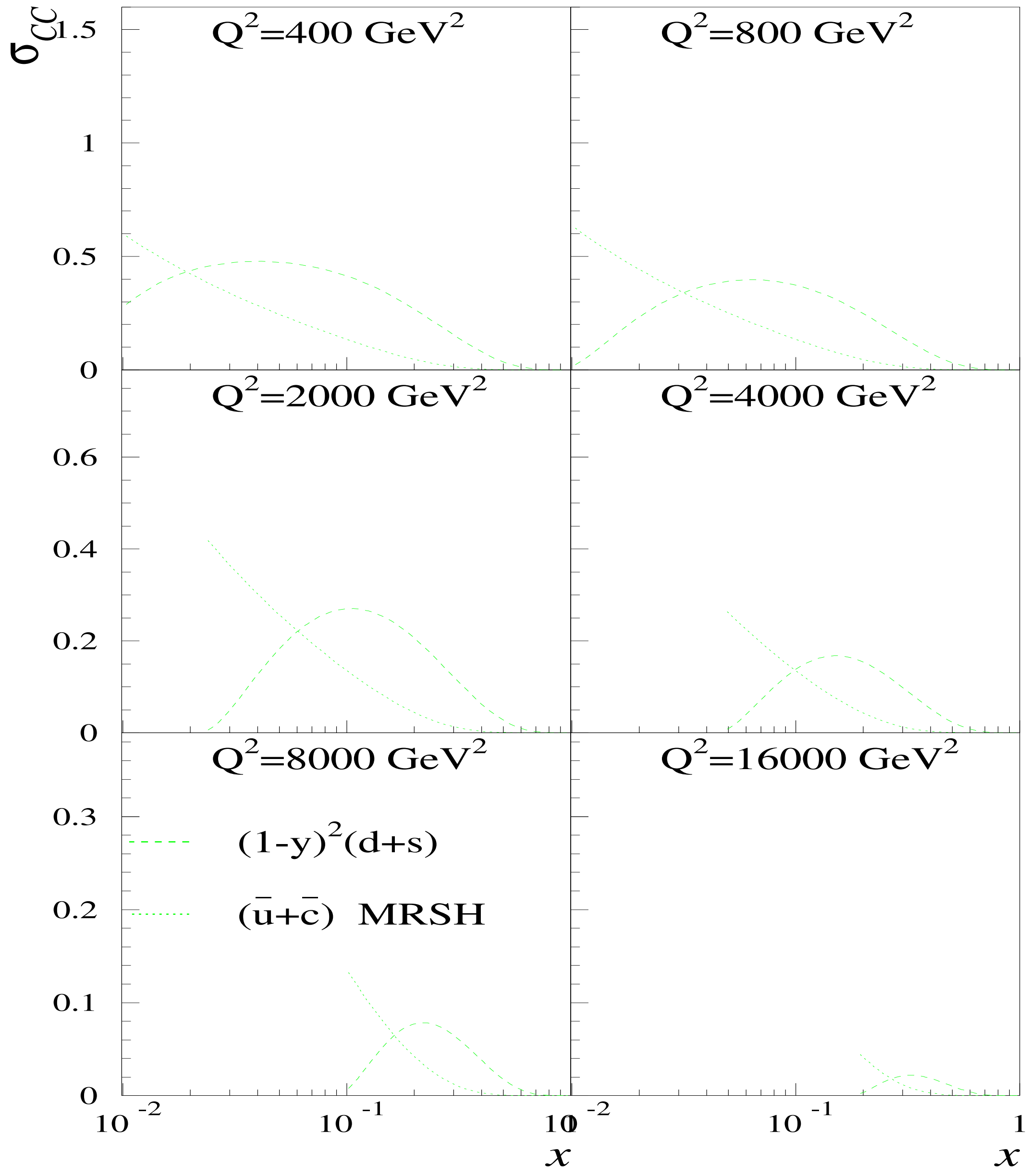


$\rightarrow$ Sensitivity to different flavours and $q/\bar{q}$

## $W$ Mass Determination (ZEUS)

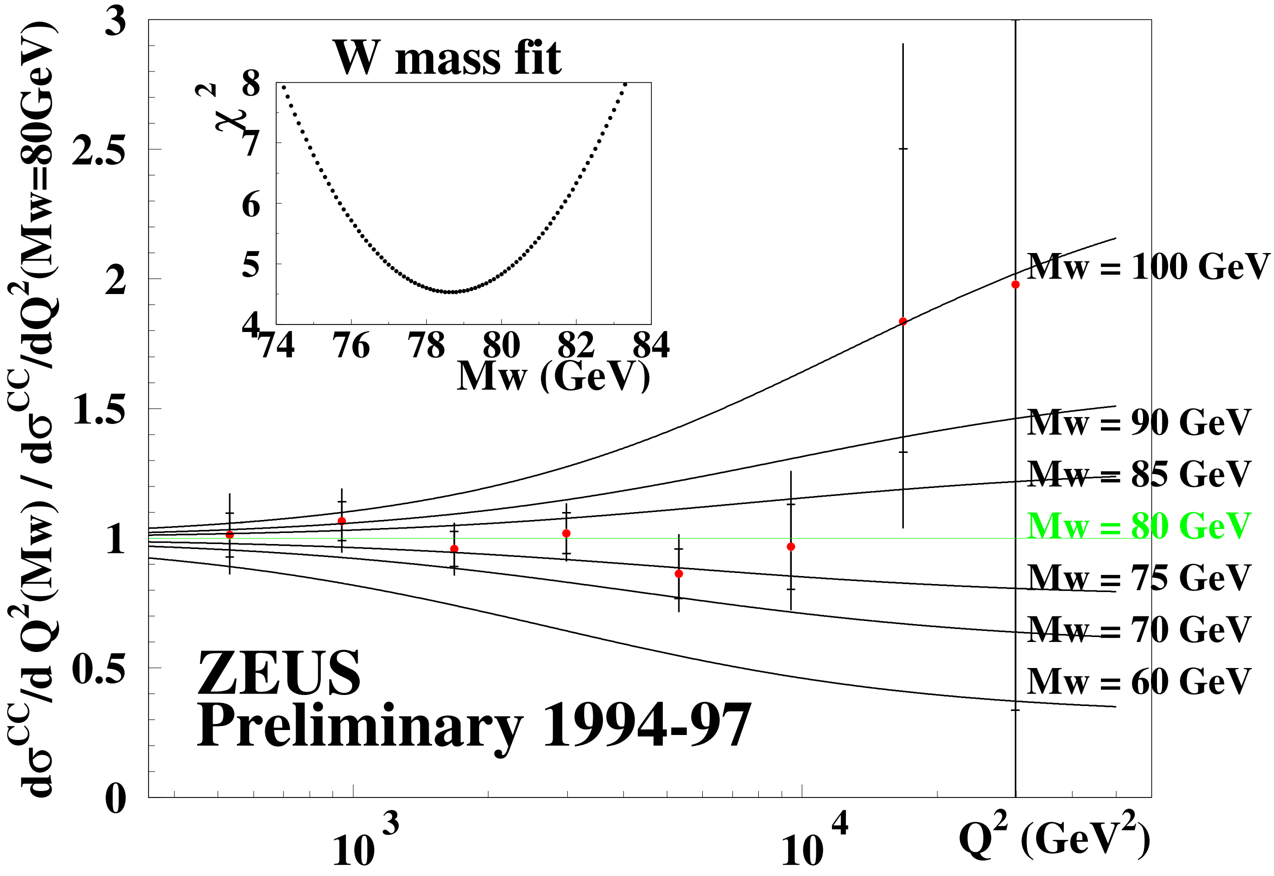


→ Determine $M_W$ from $\chi^2$–fit of theoretical prediction (with variable $M_W$) to data

$$\boxed{M_W = 78.6^{+2.5}_{-2.4}\,(\text{stat.})\,^{+3.3}_{-3.0}\,(\text{syst.})\ \text{GeV}}$$

→ Statistical error reduced by factor 3

→ Agreement with world average indicates good understanding of $E_{\text{had}}$ scale

→ Confirmation of electroweak prediction in spacelike regime

# Cross–Section Summary

- The 1994–1997 HERA data have been used for precision NC and CC cross–section measurements for $Q^2$ up to several 10000 GeV$^2$ and for $x$ as high as 0.65.

- The gap to the lower–$Q^2$ fixed–target data at high $x$ is being closed.

- All data for $Q^2 \lesssim$ 10000 GeV$^2$ show very good agreement with the SM prediction and are well described by QCD fits extending over several orders of magnitude in $Q^2$ and $x$.

- The combination of NC and CC $ep$ data in the "electroweak regime" ($Q^2 = \mathcal{O}(M_Z^2)$) promises access to PDF's of different flavours and of quarks and antiquarks.

- The high–$Q^2$ excess of NC events observed in the 1994–1996 data has not been confirmed by the 1997 data. However, both ZEUS and H1 observe a NC cross–section above the SM prediction for $Q^2 \gtrsim$ 20000 GeV$^2$. An excess in the CC data cannot be excluded.

# Scenarios Beyond the Standard Model

What if the high–$Q^2$ excess
is not a statistical fluctuation?

→ Which phenomenological scenarios explain the excess?
→ Are they compatible with other measurements?
→ How can we test them?

Two scenarios are discussed:

- Contact Interactions
  - → "Low–energy" manifestations of processes at mass scales far beyond the HERA regime
  - → Cover wide class of different processes
  - → Related to $e^+e^-$ and $p\bar{p}$ scattering and to low–energy phenomena
- Positron–quark resonances
  - → New particles coupling to $e$ and $q$ can be directly produced in $ep$ collisions
  - → Signature: resonance in $M = \sqrt{xs}$
  - → Such particles can be pair–produced in $p\bar{p}$ $\Rightarrow$ detection at Fermilab possible

# Contact Interactions (CI)

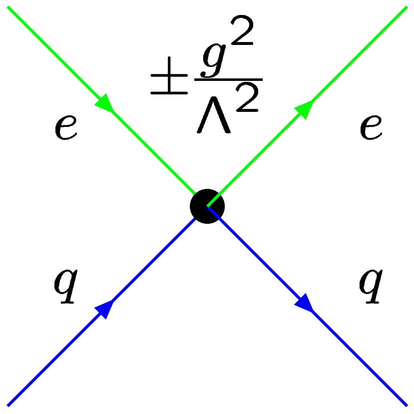


**Can represent:**

- → Heavy boson exchange
- → Leptoquark ($s$ or $t$ channel)
- → Interaction of composite electron and quark
- → ...

Historical equivalent:
4–fermion interaction

**Effective Lagrangian:**

$$\mathcal{L} = \sum_{a,b=L,R;q=u,d} \eta^q_{ab}(\bar{e}_a\gamma^\mu e_a)(\bar{q}_b\gamma_\mu q_b)$$

→ Only chiral vector couplings considered
(avoids e.g. severe constraints from $\pi$ decays)

→ Interference with SM can be constructive or destructive

**Example for cross–section modification:**

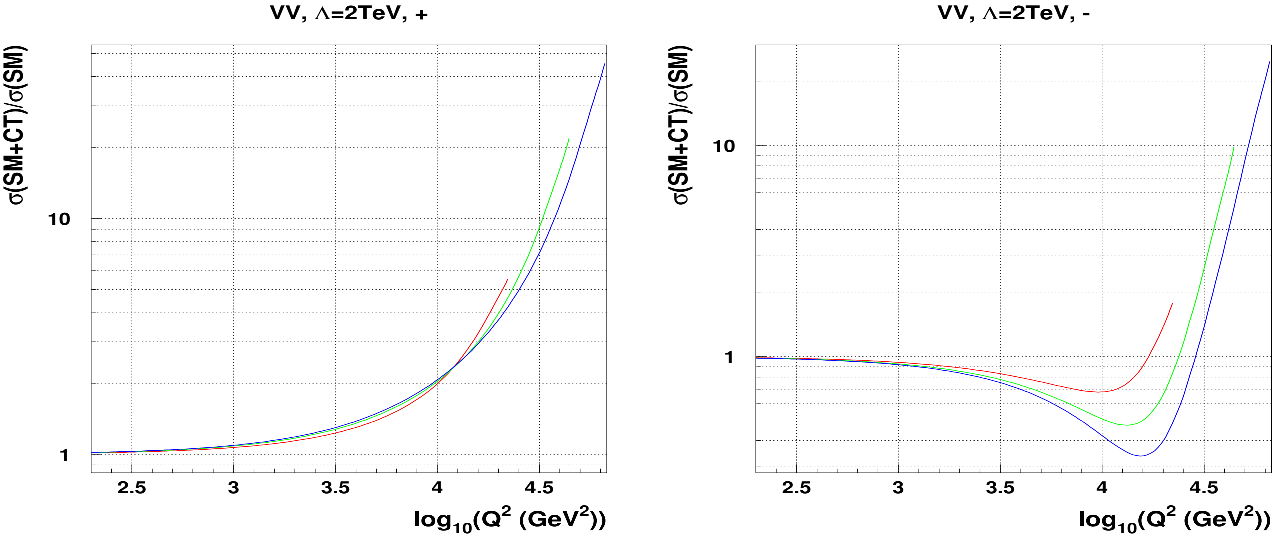

# Contact Interaction Scenarios

- CI scenario = linear combination of $\eta^q_{ab}$
  - $\rightarrow$ CI strength given by common factor $4\pi/\Lambda^2$
  - $\rightarrow$ Coefficients are taken to be $\epsilon_{ab} \pm 1$ or $0$
  - $\rightarrow$ Marginal effect if including $s, c, b, t$

| CI | $\epsilon^u_{LL}$ | $\epsilon^u_{LR}$ | $\epsilon^u_{RL}$ | $\epsilon^u_{RR}$ | $\epsilon^d_{LL}$ | $\epsilon^d_{LR}$ | $\epsilon^d_{RL}$ | $\epsilon^d_{RR}$ |
|---|---|---|---|---|---|---|---|---|
| VV | + | + | + | + | + | + | + | + |
| AA | + | − | − | + | + | − | − | + |
| VA | + | − | + | − | + | − | + | − |
| X1 | + | − | 0 | 0 | + | − | 0 | 0 |
| X2 | + | 0 | + | 0 | + | 0 | + | 0 |
| X3 | + | 0 | 0 | + | + | 0 | 0 | + |
| X4 | 0 | + | + | 0 | 0 | + | + | 0 |
| X5 | 0 | + | 0 | + | 0 | + | 0 | + |
| X6 | 0 | 0 | + | − | 0 | 0 | + | − |
| U1 | + | 0 | + | 0 | 0 | 0 | 0 | 0 |
| U4 | 0 | + | + | 0 | 0 | 0 | 0 | 0 |
| U5 | 0 | + | 0 | + | 0 | 0 | 0 | 0 |

- Several restrictions:
  - $\rightarrow$ Severe limits from Atomic Parity Violation
    $\Rightarrow$ all scenarios have $\epsilon_{LL} + \epsilon_{LR} - \epsilon_{RL} - \epsilon_{RR} = 0$
  - $\rightarrow$ $SU(2)_L \times U(1)_R \Rightarrow \epsilon^u_{ab} = \epsilon^d_{ab}$ (not U1–U5)

All CI's also modify $\sigma(e^+e^-)$ and $\sigma(p\bar{p})$

$\rightarrow$ Interference sign is different

$\rightarrow$ LEP/Tevatron and HERA have different sensitivity

# Contact Interaction Analysis (ZEUS)

- Analysis method:
  - → Input: raw distributions without acceptance or migration corrections
  - → Simulate CI's by reweighting MC events

$$\text{weight} = \left.\frac{\sigma(\text{SM+CI})}{\sigma(\text{SM})}\right|_{\text{true propagator } (x,Q^2)}$$

  - → Determine log–likelihood($\pm 1/\Lambda^2$) (LL)

Two approaches:

→ Binned LL in $Q^2$
→ Unbinned LL in $(x, y)$
→ Very similar results

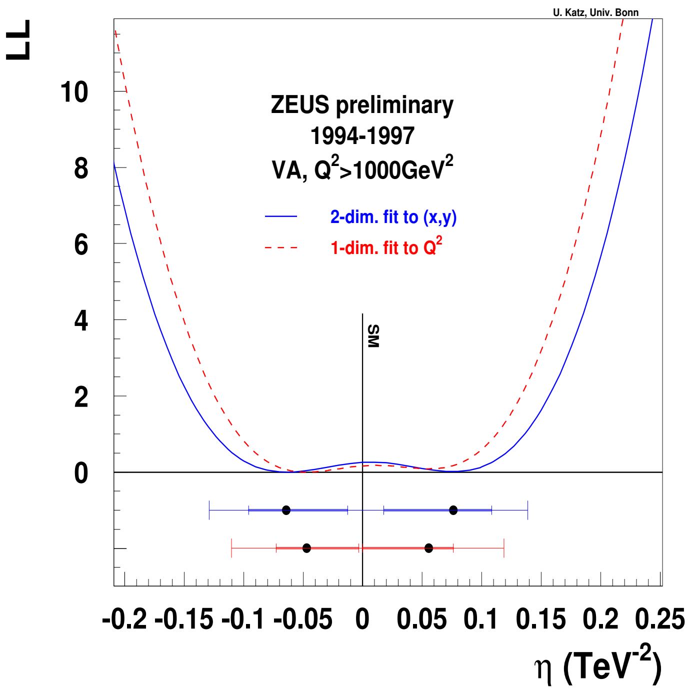


- Limit setting:
  - → Log–likelihood ⇒ best fit, 95% C.L. limits
  - → One–sided limits, probability normalised to unity for positive/negative $\eta$
  - → Cross–check with Monte–Carlo experiments

# CI Example Fits (ZEUS)

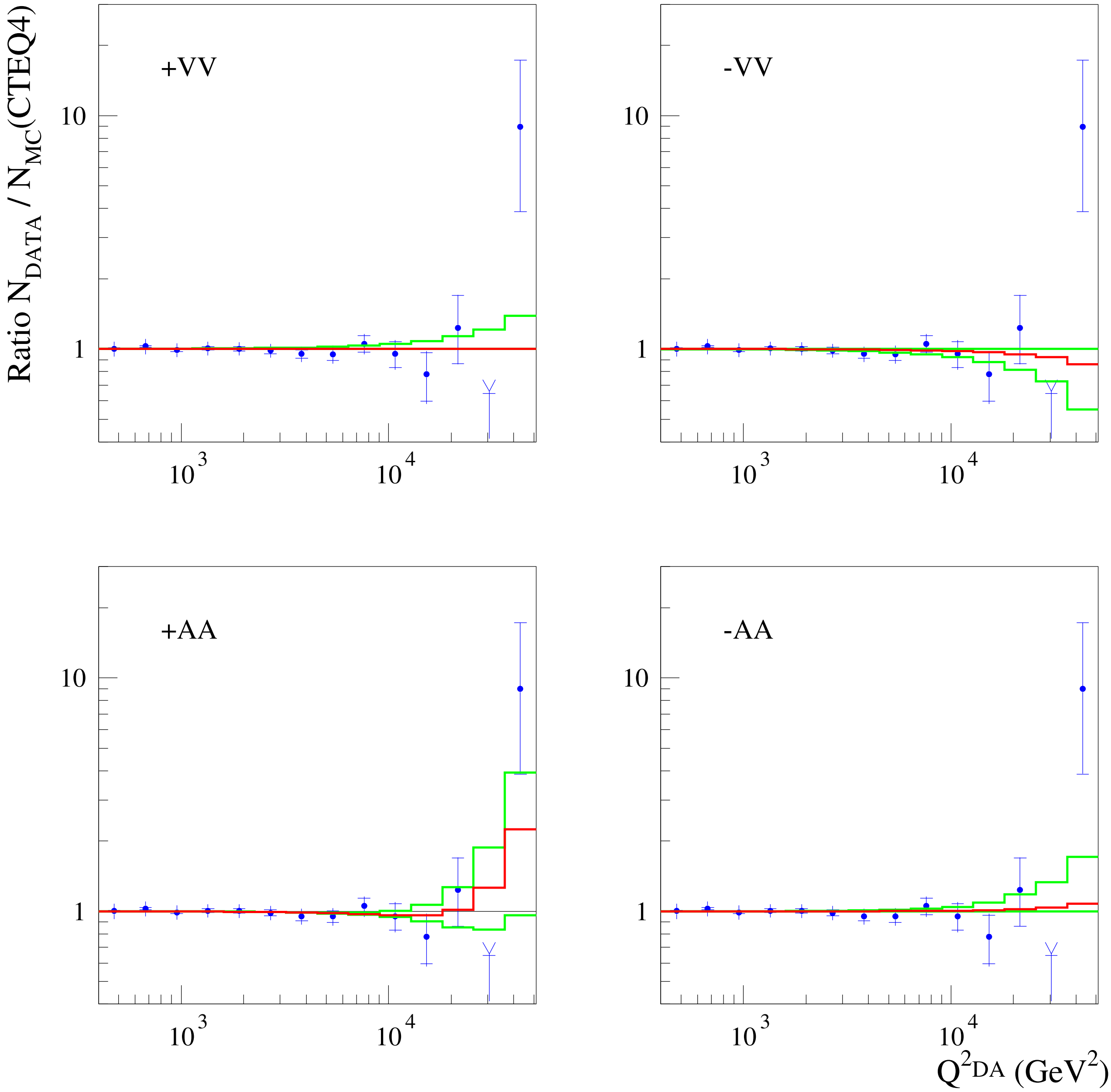


- $\rightarrow$ Points with error bars = ratio (data/MC)
- $\rightarrow$ Histograms show best fit (red) and upper/lower $1\sigma$ limits (green)

# CI Limits (ZEUS)

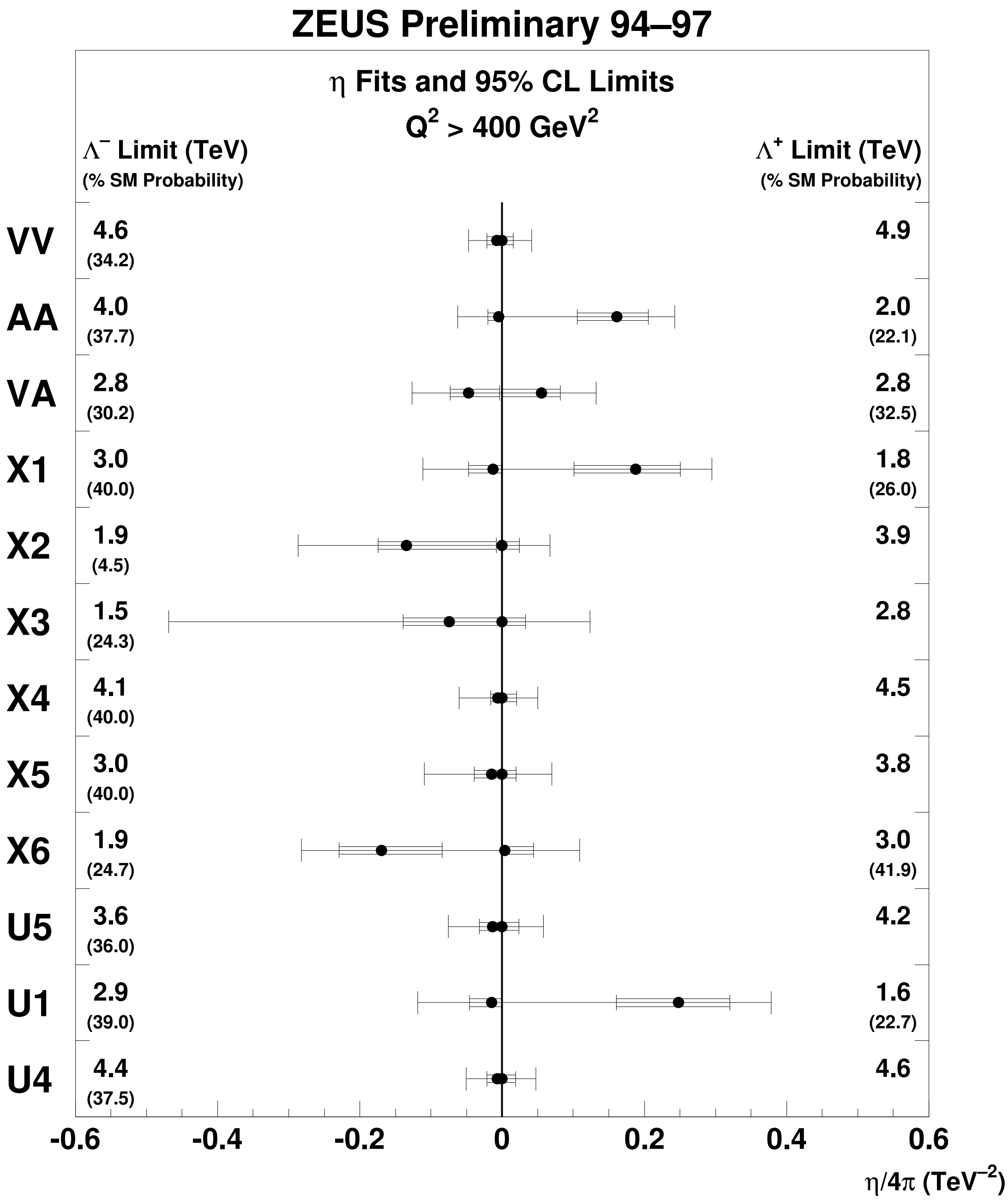


- → Dots = best fit values
- → Double bars = $1\sigma$–intervals
- → Single bars = 95% C.L. limits
- → Numbers = $\Lambda$ values from 95% C.L. limits

All CI fits compatible with SM within $2\sigma$

# Comparison to Other CI Results

| Type | **Limit from ZEUS** $\Lambda$ (TeV) | Limit from CDF $\Lambda$ (TeV) | Limit from OPAL $\Lambda$ (TeV) | Limit from ALEPH $\Lambda$ (TeV) | Limit from L3 $\Lambda$ (TeV) |
|---|---|---|---|---|---|
| $VV+$ | 4.9 | 3.5 | 3.3 | 4.0 | 3.2 |
| $VV-$ | 4.6 | 5.2 | 4.3 | 5.2 | 3.9 |
| $AA+$ | 2.0 | 3.8 | 4.9 | 5.6 | 4.3 |
| $AA-$ | 4.0 | 4.8 | 3.1 | 3.7 | 2.9 |
| $X3+$ | 2.8 | - | 3.5 | 4.1 | 3.2 |
| $X3-$ | 1.5 | - | 2.9 | 3.6 | 2.8 |
| $X4+$ | 4.5 | - | 2.5 | 3.0 | 2.4 |
| $X4-$ | 4.1 | - | 4.1 | 4.9 | 3.7 |
| $U4+$ | 4.6 | - | 2.0 | 2.1 | 1.8 |
| $U4-$ | 4.4 | - | 2.3 | 2.6 | 2.2 |

CDF Coll., F.Abe et al., Phys.Rev.Lett 79(1997)2198
OPAL Coll., K.Ackerstaff et al., CERN-PPE/97-101(1997)
ALEPH Coll., ALEPH 98-021(1998)
L3 Coll., M.Acciarri et al., CERN-EP/98-31(1998)

→ HERA, LEP and Tevatron limits are of similar magnitude

→ Some ZEUS limits are the most stringent ones

→ No obvious indication for the existence of a CI

→ CI scenarios VV and VA with $\Lambda = 3 - 4$ TeV are excluded

# Positron–Quark Resonances

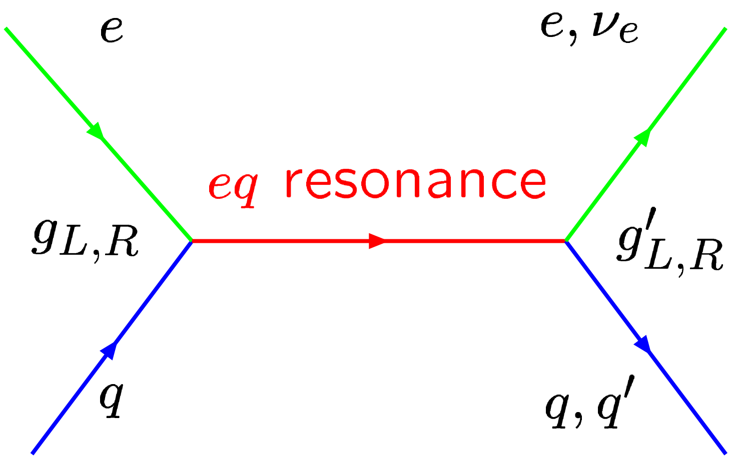


- Leptoquarks (LQ's), "classical" scheme
  - → LQ's only couple to $e$, $q$, $\gamma, Z, W, g$
  - → LQ's conserve $\mathrm{SU(2)_L \times U(1)_R}$
  - → LQ's are identified by $S$, $F$, $I_w$, $Q$
  - → $\mathrm{BR(LQ} \to eq) = 1 - \mathrm{BR(LQ} \to \nu q')$ $= 0,\ 1/2$ or 1

Only few possibilities are left by
low–eneregy and HERA $e^- p$ data:
All have $\mathrm{BR(LQ} \to eq) = 1$

- $R_p$–violating squarks ($\tilde{q}$)
  - → $R_p$–violation: SUSY particles can be singly produced
  - → Squarks can have LQ–like couplings
  - → Alternative, $R_p$–conserving decay modes $\Rightarrow \mathrm{BR}(\tilde{q} \to eq)$ can be $\ll 1$
  - → No CC–type decay modes

# Tevatron Leptoquark Limits

LQ's can be pair–produced in $p\bar{p}$ collisions

→ Cross–section does not depend on LQ coupling

→ Sensitivity decreases with BR(LQ → $eq$)

→ Stringent restiction for LQ at HERA

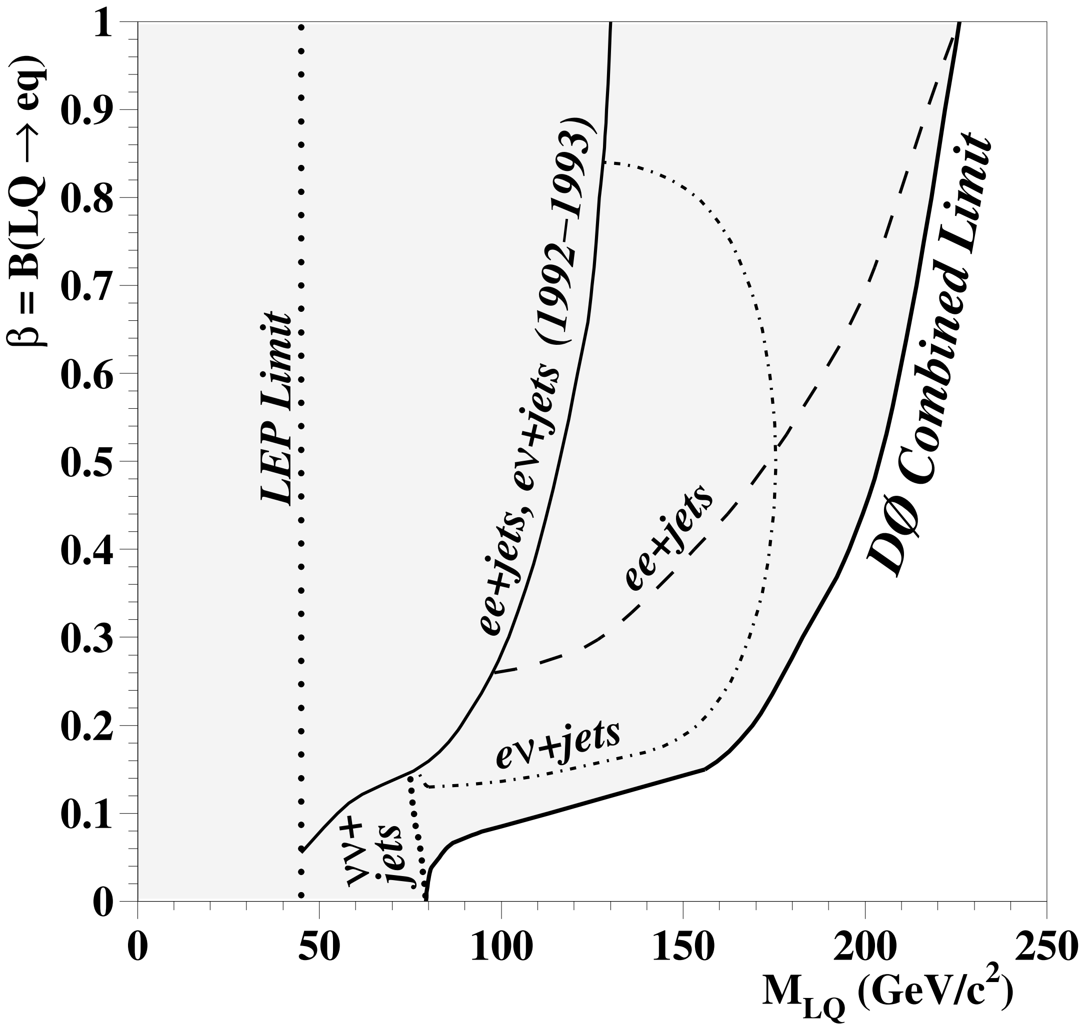


| DØ 95% lower LQ mass limts (GeV) | | |
|---|---|---|
| LQ type | BR($LQ \to eq$) $= 1$ | BR($LQ \to eq$) $= 0.5$ |
| $S = 0$ (scalar) | 225 | 204 |
| $S = 1$ (vector) | 298 | 270 |

# $e^- p$ LQ Coupling Limits from ZEUS (1993–1994)

$\lesssim 1\,\mathrm{pb}^{-1}$ $e^- p$ data suffices
to restrict $F = 2$ LQ species significantly

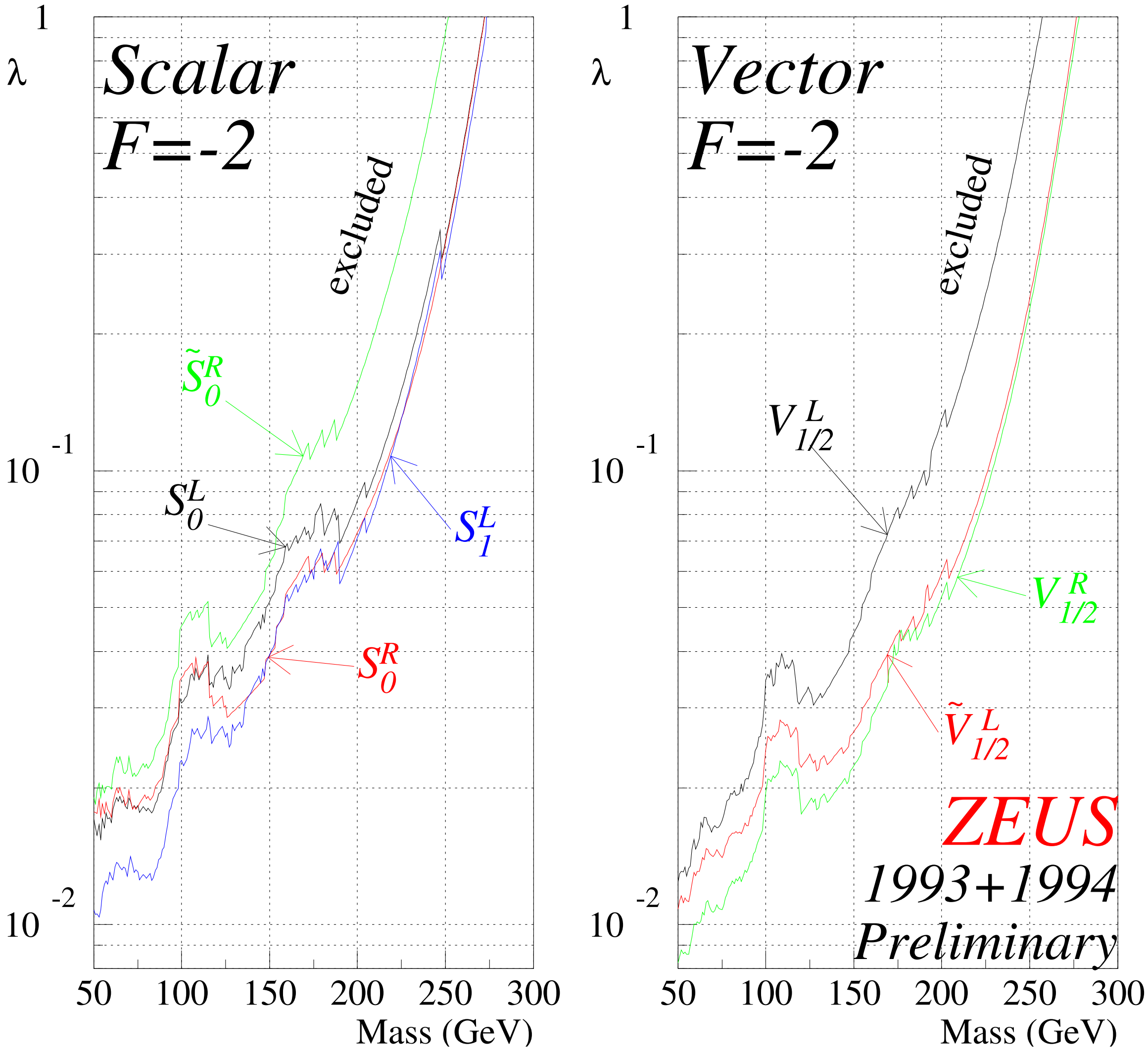


→ These limits severely restrict $F = 2$ LQ's as explanation for HERA high–$Q^2$ excess

→ Similar limits available from H1

# New LQ Limits from H1

$\sigma(ep \to \mathrm{LQ} + X)$ depends on
$M_{\mathrm{LQ}}$, coupling $\lambda$, and BR($\mathrm{LQ} \to eq$)

$\to$ Fixed $\lambda$, $M_{\mathrm{LQ}}$ limit as function of BR($\mathrm{LQ} \to eq$)

$\to$ Use Poissonian statistics in "sliding mass window"

**H1 Preliminary**

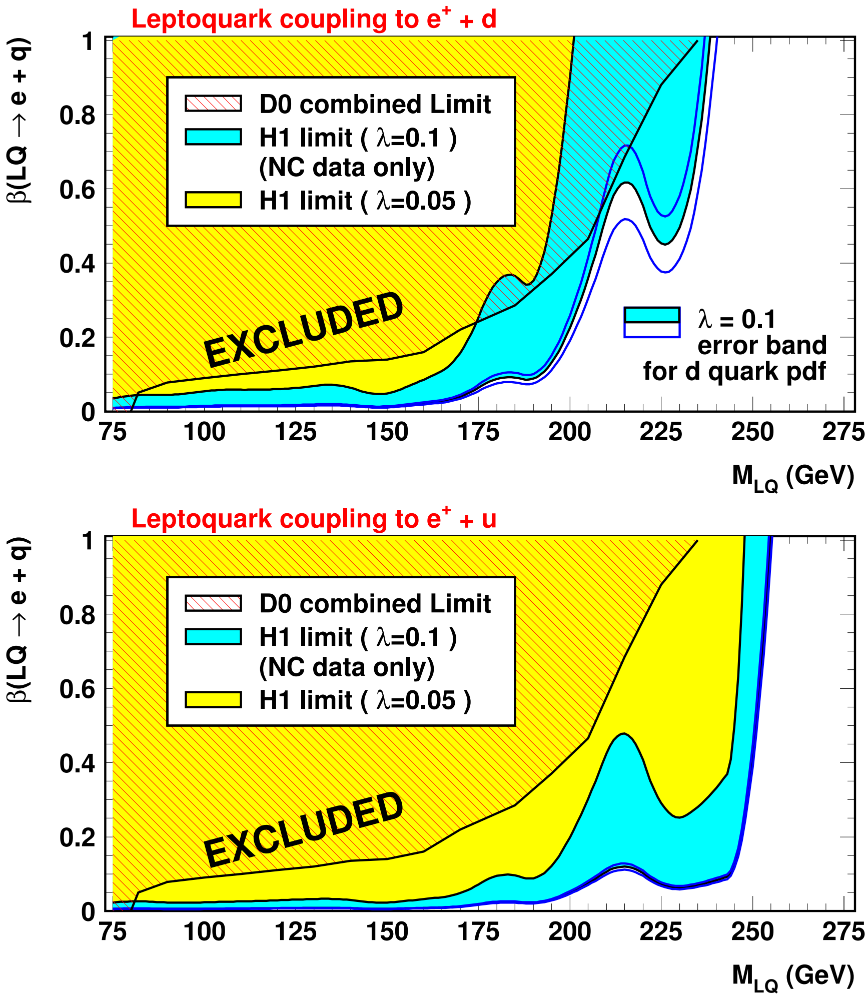


$\to$ $M_{\mathrm{LQ}} > \sqrt{xs}$ by $\sim 4$ GeV due to QCD effects

$\to$ Bump at $M_{\mathrm{LQ}} \approx 210$ GeV

$\to$ Open window at small BR($\mathrm{LQ} \to eq$)

# Conclusions and Outlook

## Conclusions

- Precision NC and CC cross–section measurements for $Q^2$ up to several 10000 GeV$^2$ and for $x$ as high as 0.65 have been presented.
- Up to $Q^2 \approx 10000$ GeV$^2$, the data are in perfect agreement with the Standard Model. QCD fits describe the data over several orders of magnitude in $Q^2$ and $x$.
- The excess at $Q^2 \gtrsim 20000$ GeV$^2$ is not confirmed in the 1997 data but is still present.
- New limits on Contact Interactions and $eq$ resonance production have been presented. No significant evidence for deviations from the SM is found. Some discovery windows for HERA.

## Outlook

- 1998–1999: $e^-p$ data at $E_p = 920$ GeV.
- After 2000: HERA upgrade: $\sim 100\,\text{pb}^{-1}$ / year
  Longitudinal $e$ polarisation

We envisage an exciting future
for high–$Q^2$ physics at HERA